SPUTTERING
OF SINGLE CRYSTALLINE COPPER
BY NOBLE GAS IONS

J. M. FLUIT

STELLINGEN

1

De door Brunnée gemeten secundaire emissie van elektronen door alkali-ionen is niet in overeenstemming met de theorie van von Roos, die de genoemde metingen bestempelt als een steun voor zijn theorie.

Brunnée, C., Z.f. Phys. **147** (1957) 161; zie § 9.
Roos, O. v., Z.f. Phys. **147** (1957) 210; zie § 5, Aussage 1.

2

Voor een zinvol massaspectrometrisch onderzoek aan neutrale deeltjes (bijv. vrije radicalen) in vlammen is het nodig een ionenbron te gebruiken waarin deze deeltjes geïoniseerd worden door elektronen met zeer lage energieën (6-20 eV).

Proefschrift A. L. Boers, Rijksuniversiteit Utrecht, 1963, hoofdstuk IV, § 5.

3

De methode van Daynes en Barrer voor het bepalen van de diffusie-constante van een gas in een metaal heeft het bezwaar dat niet tevens nagegaan wordt of het verloop van de permeatie in de tijd bepaald wordt door de diffusie in het metaal. De relatie tussen de permeatie en de inlaatdruk geeft hierover nog geen éénduidige aanwijzing. Ook de bepaling van de oplosbaarheid volgens Rogers geeft hieromtrent geen nieuwe informatie.

Daynes, H. A., Proc. Roy. Soc. **97A** (1920) 286.
Barrer, R. M., Trans. Far. Soc. **35** (1939) 628.
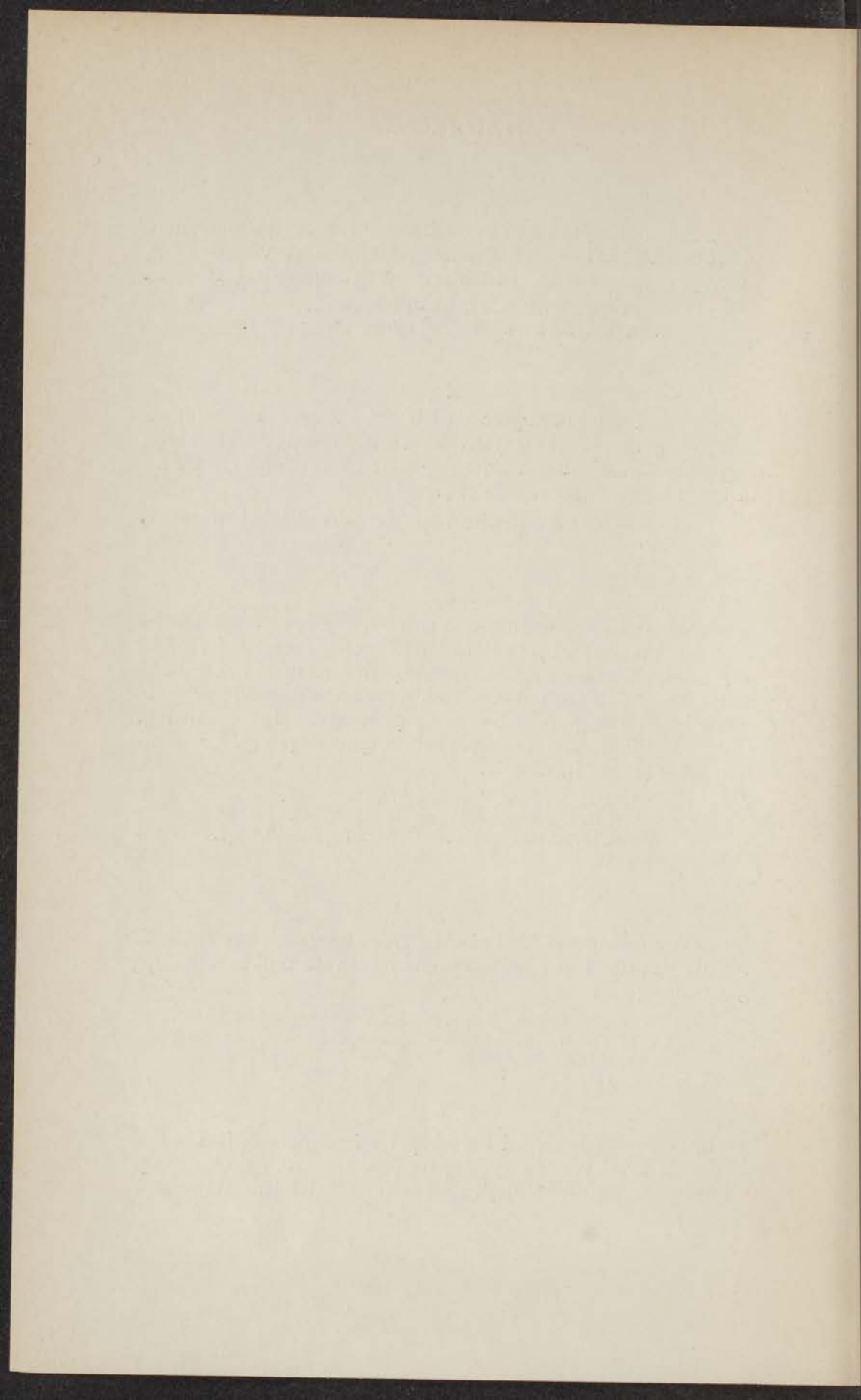Rogers, W. A., Buritz, R. S. and Alpert, D., J. Appl. Phys. **25** (1954) 868.

4

De elektronenbeweeglijkheid in mengsels van gassen kan beter als funktie van de elektronen temperatuur dan als funktie van E/p_0 gegeven worden.

Brown, S. C., Basic data of plasma physics, publishers The Techn. Press of M.I.T., John Wiley & Sons Inc., New York, and Chapman and Hall Ltd, London, p. 55.

5

De toename van de verstuiving van polykristallijn materiaal met de hoek van inval voor hoogenergetische ionen kan op eenvoudige wijze beschreven worden, als men aanneemt dat ,,direkte verstui-

ving" het voornaamste verstuivingsmechanisme is in het geval dat de ionen loodrecht invallen. Met „direkte verstuiving" wordt bedoeld dat de verstoven deeltjes veroorzaakt worden na een relatief gering aantal botsingen van het primaire deeltje.

Almén, O. and Bruce, G., Nucl. Instr. and Meth. **11** (1961) 257.
Hoofdstuk III van dit proefschrift.

6

Channeling alléén is niet voldoende om de relatief lage verstuivings-verhoudingen te verklaren, die optreden wanneer monokristallen beschoten worden met ionen in een richting dicht bij een laag-geïndiceerde kristalrichting.

Robinson, M. T. and Oen, O. S., Appl. Phys. Letters **2** (1963) 30.
Hoofdstuk I van dit proefschrift.

7

De door Wehner aangegeven mogelijkheid tot het ontstaan van dislocaties in germanium onder invloed van ionenbombardement is een vermoedelijk onjuiste veronderstelling, welke slechts ingegeven wordt door een idee dat niet door de experimenten bevestigd werd.

Wehner, G. K., J. Appl. Phys. **29** (1958) 217.

8

De berekeningen door Platkov en Illarionov over een mechanische snelheidsselector voor moleculaire bundels zijn in opzet onvoldoende en in uitwerking onjuist.

Platkov, M. A. and Illarionov, S. V., Instr. Exper. Techn. (U.S.A.) no. 2, march-april 1962, publ. nov. 1962, 353.
Hostettler, H. U. and Bernstein, R. B., Rev. Sc. Instr. **31** (1960) 872.

9

De wijze waarop Russek de statistische verdeling van de bij hevige atomaire botsing optredende excitatie-energie behandelt bevat een principiële onjuistheid.

Russek, A. and Thomas, M. T., Phys. Rev. **109** (1958) 2015.
Russek, A., Phys. Rev. **132** (1963) 246.

10

De natuurlijke reproductie van hoogmoleculaire verbindingen is niet toevallig op gang gekomen.

Bosch, L., Geloof en Wetenschap **59** (1961) 85.

SPUTTERING
OF SINGLE CRYSTALLINE COPPER
BY NOBLE GAS IONS

SPUTTERING OF
SINGLE CRYSTALLINE COPPER
BY NOBLE GAS IONS

Johannes Marius Fluit
geboren te Bussum in 1928

PROMOTOR

PROF. DR J. KISTEMAKER

Aan mijn Ouders
Aan Corrie

VOORWOORD

Met genoegen denk ik terug aan mijn MULO- en HBS-tijd in
Bussum. Mijn verdere theoretische opleiding genoot ik aan de Vrije
Universiteit te Amsterdam. Na het candidaatsexamen, richting d,
gaf ik een jaar les in wiskunde aan de Chr. HBS-A te Amsterdam,
verrichtte bodemonderzoek in opdracht van de Vrije Universiteit
en assisteerde bij het praktikum en bij een β - spectrografisch onder-
zoek.

De practische opleiding tijdens het verstuivingsonderzoek van
Dr P. K. Rol in het F.O.M. - Laboratorium voor Massascheiding
te Amsterdam was waardevol en prettig. Vanaf het begin van dit
onderzoek in 1956 tot de promotie van Dr Rol in 1960 had ik het
genoegen er aan mee te werken. In 1958 werd het doctoraal examen
aan de Vrije Universiteit te Amsterdam afgelegd. De directe leiding,
interesse en steun van Prof. Dr J. Kistemaker is steeds bij het ver-
stuivingsonderzoek van groot belang geweest; ook toen ik dit onder-
zoek voortzette. Zijn internationale contacten hadden tot gevolg
dat ik twee maal een jaar met een deskundige uit de U.S.A. mocht
samenwerken. Het in dit proefschrift gepresenteerde werk werd ook
hierdoor in belangrijke mate bepaald.

April 1963 ben ik in dienst getreden bij de F.O.M. werkgroep
massaspectrometrie die gehuisvest is in het natuurkundig labora-
torium van de Rijks Universiteit te Utrecht.

CONTENTS

INTRODUCTION

1. Sputtering

Sputtering is the ejection of lattice particles from a solid target by
ion bombardment. The phenomenon is well known in gas discharges,
where the ions hitting the cathode cause a corrosion of the cathode
and the discharge tube is coated with the sputtered cathode ma-
terial. In each apparatus where ions are accelarated to energies in
the order of 100 eV to 100 keV sputtering is observed and care
must be taken for slits and screening plates which can be destroyed
after some length of operation. The rate of damage can be expressed
by the sputtering ratio, this is the number of particles released from
the solid per impinging ion. This sputtering ratio is not more than
about unity for low energy sputtering (ion energies about 100 eV
to 1 keV) but increases with energy to optimum values between 10
and 100 for high energy sputtering (ion energies about 10 keV to
100 keV), depending on the mass of the ion and the solid under
investigation. The distinction between low and high energy sputter-
ing is only a qualitative one. It is more related to the mean pene-
tration depth of the ion in the solid. When this penetration depth
is small, say below 10 Å, the sputtered particles will for the bigger
part be caused directly by the first collisions of the ion. For deeper
penetrating ions the majority of the sputtered particles will be
ejected after a number of uncorrelated collisions. The attention will
be focused on high energy sputtering because almost all experiments
to be described in this thesis were performed with 20 keV ions.

2. Historical development of experimental techniques

The first investigations about sputtering were performed with gas
discharges by Güntherschulze, Penning, von Hippel and others.

1

They were able to establish the atomic nature of the sputtered particles. They determined a number of sputtering ratios for different cathode materials, different ions and ion energies, although the ion energies were almost exclusively in the low energy region. This means low sputtering yields. This, combined with the fact that the pressure in a gas discharge apparatus is too high (10^{-2} to 10^{-3} torr) with respect to the ion density in order to prevent surface contamination, diminishes the reliability of these measurements.

An improvement on this technique was made by Wehner: the ions were drawn electrically from the gas discharge by which it was possible to reach a pressure of 10^{-4} torr around the target. A comparable apparatus was used by Koedam. The acceleration of the ions could be increased (but remained below 10 keV) and a better determination of the angle of ion incidence was possible. A lot of useful sputtering data could be obtained. Some topics may be mentioned:

1. the increase of the sputtering yield with the angle of ion incidence (defined relative to the surface normal) was measured;
2. the sputtered atoms ejected from single crystals showed preferential directions along low index crystal axes;
3. a preferential direction for very low energy sputtering of polycrystalline metals was found to be normal to the ion direction;
4. special surface patterns were observed after the erosion by the ion bombardment, not only preferential etching of grain boundaries, but also special hillock and pit formation depending on the orientation of the grains.

Another step forward in the experimental technique was the use of a separate ion source from which the ions were drawn by an accelerating system and analyzed and focused by a magnetic field. By this technique it is possible to get ion beams of about 10 mA which are extremely pure (well defined ion mass). The ions can be accelerated to energies in the whole region of interest and the pressure can be 10^{-6} torr. The current density is then at least of the same order of magnitude as the density of particles arriving at the target from the rest gas, wich could cause contamination of the surface. The sputtering action itself takes care of the maintaining of a clean surface. The electromagnetic isotope separator, developed in and after the second world war, is an apparatus which has essentially the features mentioned above. Indeed the use of these apparatus was the next step forward in the research about sputtering. Rol (Amsterdam), Almén and Bruce (Gothenburg), Yonts and Southern (Oak Ridge) and Perovic (Belgrado) used an isotope separator and gathered a lot of reliable sputtering data on different combinations of ions and metals. Rol found the influence of the chemical binding

on sputtering by using only polycrystalline copper and bombarding with ions of many elements. Those ions which are expected to form stable compounds with copper, revealed a binding influence by a relatively low sputtering rate. The sputtering yields of the ions which did not react with copper (especially noble gas ions) were determined as a function of energy and could be explained reasonably well by taking into account only the mean penetration of the ion into the solid. The result of this discovery will be discussed further at the end of this introduction when we start to discuss some underlying ideas of the work presented in this thesis.

Almén and Bruce extended the work of Rol to other metals and confirmed his conclusions. Moreover, they established that a high penetration depth is also correlated with a high saturation value of the amount of the injected material in the target. Perovic, Yurasova and Southern (Robinson) measured preferential ejection along low index crystal axes, also in the case of high energy sputtering. It was possible to measure the directional distribution of the particles ejected around these directions. Nelson (Thompson) built an apparatus especially intended for sputtering experiments with the essential features of an isotope separator, but with still better vacuum conditions at the target (10^{-7} torr) attainable due to good focusing properties of the ion beam. They were able to make accurate measurements of the directional distribution of the ejected particles as a function of target temperature. They built a fast rotor in the high vacuum compartment and measured the velocity of the sputtered particles for different directions of the ejected particles. Nothing was said so far about the velocity of the ejected particles, for the earlier measurements concerned only mean velocities. We will see in the next section that this has only a very limited value. Only measurements of velocity distributions for the preferential direction of ejection occuring during single crystalline sputtering will give further basis to the present ideas about sputtering.

3. Sputtering mechanism

We want to discuss now some special features of the mechanism causing high energy sputtering to elucidate the present status of the subject. In the 10 to 100 keV region the energy loss of the ion can be described quite well as being transferred in collisions with single atoms. One of the most adequate potentials used to describe the interaction between a lattice atom and the fast ion is the Bohr potential

$$V = \frac{Z_1 \, Z_2 \, e^2}{r} \exp\left(-\frac{a}{r}\right).$$

3

This is a Coulomb potential for an internuclear separation r in which an effective screening length a (a few times 0.1 Å) is introduced to describe the repulsion of the electron clouds when the particles collide with medium velocities. At much higher velocities is the interaction of the separate electrons of the collision partners most important and the energy transfer to the electrons is not used for the displacements of lattice atoms (necessary for sputtering), but for electronic excitations. On the other hand slow projectiles (energy below 100 eV) interact with more lattice atoms at the same moment and sputtering is again less probable for it is necessary to transfer about 25 eV to one atom in order to displace that lattice atom in a normal metal.

This 10—100 keV energy region is thus the most effective region to cause displacements of lattice atoms. This can be seen e.g. in photographic emulsions where nuclear particles describe straight lines till their energy is low enough to cause displacements. The path of the projectiles becomes zig—zag (straggling) and ends after a relative short distance (order of magnitude some 100 Å). This is the lattice region where permanent damage is made and which is detected in radiation damage experiments by their local increase of electrical resistivity. When the primary energy of the projectile is low enough, so that this damage region with displacements starts right at the surface, sputtering occurs. It is then quite reasonable to put the sputtering ratio S proportional to the primary energy E (for the number of displaced atoms is in first approximation proportional to E) and inversely proportional to the free pathlength of the bombarding ion in the lattice of the metal under investigation. The extension of the displacement zone increases mostly in forward direction for higher primary ion energies, which means that S decreases because of the deeper position of the whole displacement zone. Rol was able to fit his experimental $S(E)$-curves quite well to this behaviour of the displacement zone.

At the moment machine calculations are most promising for an accurate determination of the possible collision sequences in a solid. Nevertheless, it is still impossible to calculate total sputtering ratios with a reasonable accuracy, for a suitable interatomic potential for all energies involved during the slowing down process is not yet at hand. Moreover, the lattice vibrations could not yet been introduced in the machine calculations. However, important results have been reached. We mention the *channeling* mechanism (Robinson, Leibfried). Particles with an energy of some keV travelling into a direction almost parallel to a low index crystal direction proceed into these directions over long distances (100—1000 Å). As a result of the mild potential variations in the middle of the canal the particles follow a sinusoidal path between the surrounding atom rows with periods of more than 10 Å. Only a few percent of all possible

4

directions are suitable for channeling, but the influence on the extension of the displacement zone is, nevertheless, important. It is also important for at least a partial explanation of the fact that all damage theories overestimate the damage. The loss of energy in a chanelling event consists of small amounts of energy to each lattice atom along its path and displacement does not occur as long as the particle remains in the middle of the channel.

The last two conclusions regarding the bigger extension of the displacement zone and the smaller amount of the displacements are also valid for other focusing collision sequences. One of the other focusing collision mechanisms is the *ring-* or *lens-* or *assisted focusing*, which causes e.g. the ejection of particles in the [100] directions of a f.c.c. lattice. The potential distribution of four adjacent [100] atom rows can act as a series of lenses. Particles with about 100 eV energy passing through these rings of atoms are focused toward the [100] direction. This focusing mechanism can also be applied to the particles in a [111] direction of a f.c.c. lattice, but the amount of particles focused into that direction is smaller because of an asymmetry in the successive lenses. The most dominant *focusing* in f.c.c. metals is along [110] axes. During these collisions the impuls is propagated along the atom row itself. The particles involved in such a collision sequence fall back to their original lattice site. If the collision sequence reaches the surface, the surface atom is mostly kicked off (the displacement energy is about 25 eV, but the surface binding energy is only 5 eV). The focusing is due to the directional correlation between successive collisions in the row. This is the dominant behaviour for collisions in a solid when low energies are involved (<100 eV). For at these low energies the struck atoms must receive their momentum from one of its nearest neighbours and passage between lattice atoms is impossible because of the large collision cross-sections for these low energies. The reason that just such low energy particles are important in sputtering is the following. Firstly, the number of particles with low energy is bigger in a collision cascade and secondly, the possible modes of reversing the impuls from the original direction of the ion, normal to a crystal surface, increases with the number of collisions. The average energy of the sputtered particles is almost independent of the primary ion energy. The value is of the order of 10 eV.

Thompson measured the velocity distribution of the particles ejected along [110] and [100] directions of a f.c.c. lattice. He was able to determine the maximum energy for which focusing along a [110] direction is possible. There was a broad distribution of particles with energies below the maximum focusing energy and a small tail in the thermal region (which is one of the best proofs of the inadequacy of the old evaporation theories). A very small contribution was also measured above the maximum focusing energy. This must

be due to channeled atoms. The spectrum for particles ejected along the [100] direction was different. A sharp cut off at an energy above the displacement energy showed clearly that in this case displacement collision sequences must be involved.

4. The experiments described in this thesis

The importance of the penetration depth of the ion in the metal with respect to the total sputtering ratio can be checked further by measuring total sputtering ratios of single crystals by bombarding in different crystal directions. In the open directions (low index crystal directions) relatively low sputtering ratios are expected. These measurements will be described in chapter I.

The special structure of surfaces bombarded by ions was already mentioned. There is no satisfactory explanation for the development of this micro relief. An attempt to such an explanation was made by an investigation, which was initiated by the measured influence of the micro relief on the total sputtering ratio. A possible correlation with the penetration depth of the bombarding ion was again the underlying idea. The light reflection measurements of ionically bombarded copper single crystals to reveal the surface relief are described in chapter II and the results show indeed the possibility of such a correlation.

In soft collisions of energetic ions with lattice particles, very small amounts of energy are transferred almost perpendicular to the direction of the ions. This can cause sputtering of surface atoms perpendicular to the ion beam for oblique incidence. This mechanism was first proposed by Datz. Experiments to investigate this low energy sputtering component during high energy sputtering experiments are described in chapter III.

It was already stated that machine calculations of collision processes in solids do not take into account the lattice vibrations. This also is the case with most of the published analytical calculations. Therefore, it will be very important to measure the influence of lattice vibrations by performing experiments at low target temperature. In chapter IV measurements of sputtering ratios at low target temperature are reported. Sanders developped an analytical theory to calculate the influence of lattice vibrations on focusing collision sequences. The consequences of the results of this theory for the total sputtering ratio at various lattice temperatures is discussed. Chapter V describes reflection measurements. Friedman proposed surface ionization as a method for detection of sputtering particles in order to reduce the rather long bombardment time involved for a determination of the sputtering ratio. This turned out to be impossible because of the large number of reflected incident ions for

more oblique ion incidence. A study of the reflection phenomenon was made because of its close relation to sputtering. The reflected particles arise from single collisions with lattice atoms in the first two or three layers. Their energy is much higher than the energy of the sputtered particles. The amount of reflected particles can be as much as 10% of the incident ions. It will be shown that the reflected particles can influence the micro structure of the ionically bombarded targets by secondary incidence.

This introduction is not intended to give credit to all workers in the field of sputtering. It is merely a number of facts and thoughts to introduce the experimental chapters. Stresses on certain features and choices of mentioned names reflect only the writers personal acquaintancy. The corresponding literature can easily be found in the references of the following chapters.

A recommended review article is that from G. K. Wehner: Sputtering by Ion Bombardment, Advances in Electronics and Electron Physics VII, ed. L. Marton, Acad. Press, New York, 1955, p. 239. An extensive literature research about sputtering will be published by R. Behrisch, Automn 1963, in "Ergebnisse der Exakte Naturwissenschaften".

ANGULAR DEPENDENT SPUTTERING OF COPPER SINGLE CRYSTALS BY 20 keV NOBLE GAS IONS

1. *Introduction*

Sputtering is the phenomenon of ejection of lattice atoms caused by an impinging ion. The sputtering ratio is the number of particles released per impinging ion. This ratio is a function of many parameters including the energy E and atomic mass M_1 of the incoming particle, the atomic mass M_2 and the structure of the bombarded metal. It was shown[1]) that it is possible to describe the dependence of the sputtering ratio, S, on these parameters in the framework of the Bohr theory of atomic collisions[2]) by the formula

$$S = K \frac{M_1 M_2}{(M_1 + M_2)^2} \frac{E}{\lambda(E)}$$

where $\lambda(E)$ is the mean free path of the ion with energy E, calculated from the screened atomic potential as used by Bohr, for the solid under investigation. $EM_1 M_2 / (M_1 + M_2)^2$ is proportional to the elastic energy loss of the ion in the first collision with a lattice atom. The constant K was determined by fitting the experimental data to the equation. The value obtained for polycrystalline copper for many different (chemically inert) ions in the energy region from 5 to 20 keV was $K = 1.7 \times 10^{-11}$ m/eV[1]), in agreement with the K-values found by Almén and Bruce[3]) for different 45 keV noble gas ions on copper. It is the purpose of this chapter to extend this description of sputtering phenomena by a study of the angular and structural dependence in order to get a better understanding of the penetration of high speed particles into solids.

The influence of the angle of incidence was recognized by Fetz[4]), for the case of polycrystalline molybdenum. Upon diminishing the diameter of molybdenum wires in a low pressure mercury plasma, an increasing sputtering ratio was observed which was explained by the increase of the average angle of incidence. Quantitative

experiments were done at our laboratory with Ar^+ and Tl^+ ions on polycrystalline copper at 20 keV for incidence angles φ (defined with respect to the normal) ranging from 0 to 50°[5]).

Both species of ions gave a monotonic increase of the sputtering yield, which could be described with the empirical formula:

$$S(\varphi) = S(o) \left[\frac{2}{\cos \varphi} - 1 \right].$$

Wehner[6]) studied the sputtering of small polycrystalline spheres, which were sputtered by a parallel stream of Hg^+ ions of low energy (125 — 800 eV). $S(\varphi)$ was determined by measuring the thickness of the material removed from different spots on the spheres.

Although Wehners results describe sputtering at low energy they appear to be in approximate agreement with the higher energy values.

1. He found that several groups of metals displayed different behaviour in the magnitude of the effect of incidence angle on sputtering. The group Cu, Ag, Au, (Pt) gave the smallest effect.

2. This metal group showed, on the other hand, a relatively high sputtering ratio.

Therefore these metals are most adequate to find a relation between the sputtering yield and the structure of metals.

The advantages are:

a. When the change in S with angle of incidence is small for the polycrystalline material, then for single crystals this change will be mostly a consequence of the change of the crystal orientation with respect to the beam direction.

b. The relatively high sputtering ratio is an advantage for the accuracy of the measurements.

c. There will be a negligible chemical influence, because of the chemical inactivity of these metals, especially when noble gas ions are used as the bombarding ion[5]).

d. The interpretation of results with a hard sphere model will be more justified for these metals which have closed d - shells.

Although the mentioned results on polycrystalline material give some information about the sputtering process we believe that it is necessary to understand first the sputtering of single crystals before it will be possible to give more conclusive arguments for the sputtering mechanism. The sputtering of single crystals showed a remarkable difference, in all respects, with that of polycrystalline material for both low energy[7,8]) and high energy ions[9]).

It may be thought questionable that we can treat a single crystal under bombardment as an ideal crystal in the region where the ion bombardment influences the crystal (i.e. *ca* 300 Å depth for 20 keV

Ar⁺ on Cu). Although we want to discuss possible changes in this crystal region at the end of this chapter, we should like to point out here firstly that the X-ray diffraction patterns remain unchanged after prolonged bombardment and secondly that Ogilvie[10] found from electron diffraction patterns of Ag targets bombarded with 4 keV Ar⁺ ions *only* a disorientation of surface crystallites about 100 Å thick, which are turned a few degrees around the [112] axis. It may also be noteworthy that Laponsky and Rey Whetten[11] reported a similar dependence on crystal orientation (as those shown in section 3) for secondary electron emission, although the proposed explanation[12] is quite different from that for sputtering, given in this chapter.

Our preliminary experimental results about the influence of crystal orientation on the sputtering yield were presented at the IVth international conference on ionization phenomena in gases[9]. They were followed by the investigation of Almén and Bruce[3] who measured also variations in sputtering yield due to crystal orientation. We present now in the next sections an extended and revised version of the description given in a paper in the J. Appl. Phys., 34 (1963) 690.

2. *Experimental procedure*

The single crystalline copper targets*) were bombarded at the collector side of an 180° electromagnetic isotope separator with noble gas ions at an energy of 20 keV. The target is pressed with a graphite diaphragm to a copper plate. The graphite diaphragm is carefully shielded from the ion beam. The target is cooled at a constant rate, such that the temperature can rise to approximately 100°C for the highest currents (600 μA for normal incidence). Because of the decrease in target current at higher angles of incidence, the target temperature will also decrease, but the corresponding change in sputtering can be neglected[13]. The sputtering ratio was determined from weight loss and integrated current measurements. Due to the presence of the magnetic field in the collector region and a negative potential on the collector, neither electrons from the beam, nor secondary electrons from the target can influence the current measurements[5]. The current density of about 100 to 200 μA/cm²

---

*) A copper single crystal was prepared by melting copper in a cylindrical graphite mould tapered at one end and cooling the melt from this end (performed at the Natuurkundig Laboratorium van de N.V. Philips, Eindhoven). Specimen of the desired orientation were cut from the single crystal with a jewelers saw and smoothed on a milling machine. The surface to be bombarded was polished electrolytically (about 0.2 mm was removed). Its final orientation was accurate within 2°, as determined by ordinary Laue methods (performed by Dr. M. de Jong of the Natuurkundig Laboratorium van de Universiteit van Amsterdam).
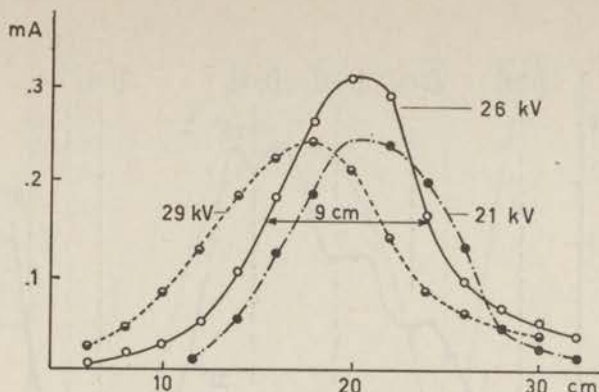
Fig. 1. Profile of the 20 keV ion beam after 90° deflection. The current, measured on a plate of 2 cm width, is given as a function of the distance from the outer wall of the vacuum-chamber. Different curves correspond to different extraction voltages.

for normal incidence was high enough to prevent the formation of impurity layers. This is only true if the angle of incidence is kept below $\approx 70°$, for it was shown on polycrystalline copper (for which $S = 6.5$ when 20 keV Ar$^+$-ions were used) that a current density below 10 μA/cm^2 is too low to give reliable values for the sputtering ratio.

Of course, these remarks on possible formation of impurity layers which interfere with sputtering are only valid for the collectorside of the separator, where the ambient gas consisted of noble gas at a pressure in the order of 10^{-5} torr and a background pressure of about 10^{-6} torr.

The crystal surfaces exposed to sputtering were (100), (110) and (111) surfaces. We varied the incidence angle for the (100) and (110) crystal by turning these crystals around an [010] or [011] direction in the surface. Measurements of the aperture of the beam were done in the middle of the separator, i.e. after 90° deflection. The measured beam shapes for different negative extraction voltages are given in fig. 1. The curve which is valid for the 26 kV extraction voltage (final beam energy 20 keV) corresponds with the maximum beam intensity after 180° deflection. The half width of 9 cm corresponds, in the 1 m radius separator, with an angular interval of 3°. Because of this, measurements of the sputtering ratio were made at every two degrees of angle.

The direction at which the ions enter the collector region of the isotope separator is influenced by the focusing properties of the magnetic field. The direction in which the maximum beam intensity
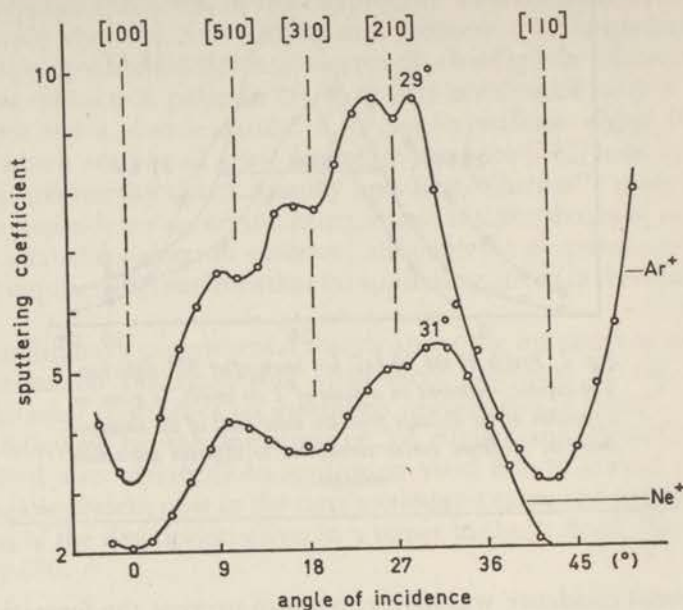
11

Fig. 2. *The sputtering ratio for a (100) surface of a copper crystal, which is rotated about an [010] direction in the surface. The 20 keV bombarding ions are Ar⁺ and Ne⁺.*

strikes the crystal after 180° deflection is measured separately by putting slits in the beam path. In the results of the angular dependence measurements, as given in the next section, we have corrected for the angular deviations caused by the inaccuracy in the cutting procedure of the single crystals.

The relative error in some measurements of one sputtering ratio at a fixed angle of ion incidence is about 3% when the orientation of the crystal is not changed with respect to the ion beam in between. This is also the case for measurements at angles of incidence which are not more than some degrees apart. This means that surface irragularities cause a less important error in the behaviour of sputtering ratio *vs* angle curves than the angular spread of the ion beam. The quantity of copper removed for every measured sputtering ratio was about 1 mg/cm², which was enough to give a weighing accuracy in the order of 1%.

The error in the absolute value of the measured sputtering ratios caused by surface irragularities is in the order of 10%.
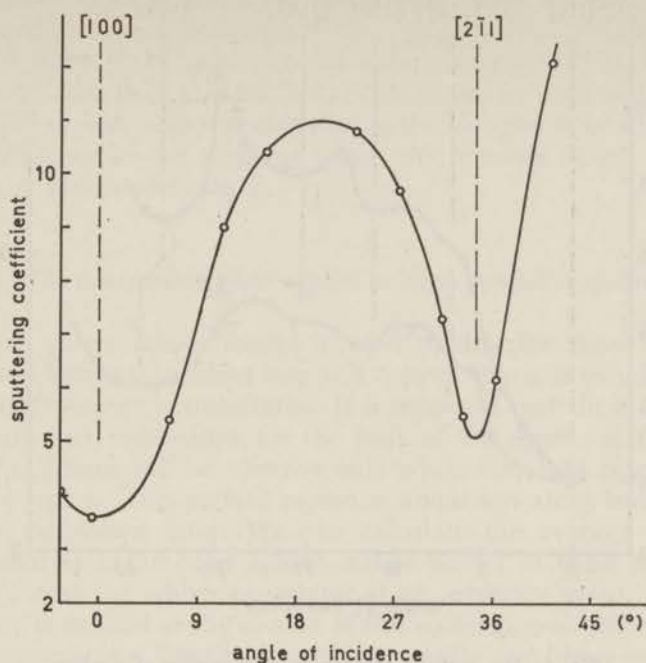
12

Fig. 3. The sputtering ratio for 20 keV Ar+ ion bombardment on a (100) surface of a copper crystal, which is turned around an [011] direction in the surface.

3. Results of sputtering ratio measurements

The measured sputtering ratios for the (100) crystal (i.e. a copper crystal cut so that the bombarded surface coincides with a (100) plane), which is bombarded along different crystal directions in an (010) plane are shown in fig. 2.

When the crystal is rotated about an [011] direction in the surface, the variation in sputtering ratio differs from that in the former case (cf. fig. 3). In this case[9]), however, not enough data were taken to detect small minima as seen in fig. 2.

We emphasize once more that we used angular dependent measurements to determine the influence of crystal orientation, without using a set of crystals with different surface orientation. By choosing a (110) crystal and rotating about an [001] direction in the surface, we are able to see the influence of angle superimposed on the orientation effect. In this case the crystal directions from 0° to 45° are the same as those from 45° to 0° in the case of the (100) crystal
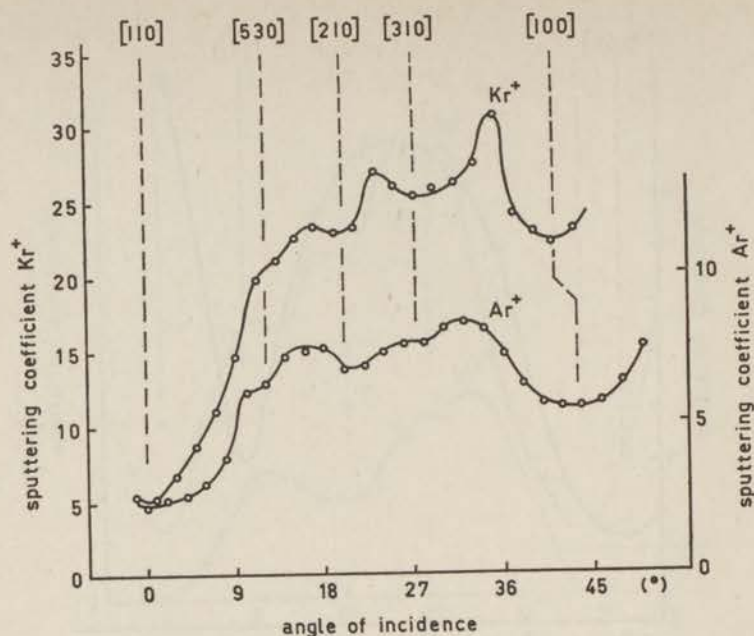
Fig. 4. The sputtering ratio for a (110) surface of a copper crystal, which is turned around an [001] direction in the surface. The 20 keV bombarding ions are Kr⁺ and Ar⁺.

rotated about an [010] axis. The results of the measurements with the (110) crystal for Ar⁺ and Kr⁺ ion bombardment are given in fig. 4.

We did some spurious measurements of the sputtering ratio of a (111) copper crystal with 20 keV Ar⁺ ions showing that the high value measured for normal incidence, namely 8.2 was also a relative minimum. S was 9 for φ equal to 6° or 8°. The results of the measurements given in fig. 2, 3 and 4 can be summarized as follows:

1. Relative minima in S are found for ions penetrating along low index crystal directions namely the [100], [310], [210], and [110] directions. There are also indications for a minimum along the [510] direction when a (100) crystal is used and a minimum along the [530] direction when a (110) crystal is used. These directions are shown in fig. 5. Possible deviations between the orientations indicated in fig. 2, 3 and 4 and the exact values for the angle of incidence at which these indications should be are within the experimental errors.

2. Rotating a (100) crystal about an [011] axis in the surface gives,

14

as a mean, higher sputtering ratios than when the same crystal is rotated about an [010] axis.

3. The deep [110] minimum at approximately 45° in fig. 2 for Ar+ is broader than that for Ne+. Some measurements with Ar+ on the (100) crystal were repeated during the Ne+ run to be sure about the difference in the angle at which the maxima at 29° and 31° occur, as indicated in fig. 2.

4. *The transparency model applied to single crystalline sputtering*

A hard sphere lattice model is used to describe those collision processes between incident ions and copper atoms in which a large amount of energy is transferred. It is supposed that these collisions are indirectly responsible for the bulk of the sputtered material. These collisions will be effective only when they take place in the surface region. This surface region is about ten atom layers thick as will be shown later. We can calculate the average collision probability for the hard sphere lattice model in these ten atom layers for an ion which penetrates at an arbitrary point. A transparency is defined as the inverse of this collision probability. Thus, high transparency implies deeper penetration and lower sputtering yields. The transparency is a function of the crystal direction along which an ion penetrates. This function shows pronounced maxima at low index crystal axes, because of the deep penetration for ions aimed along these axes. The radius of the spheres in this lattice model is different for different mass and energy of the projectile. This radius has been calculated from a suitable inter-atomic po-

Fig. 5. *The directions where minima in sputtering occur, shown in the (001) plane perpendicular to the surfaces of two crystals which were used.*
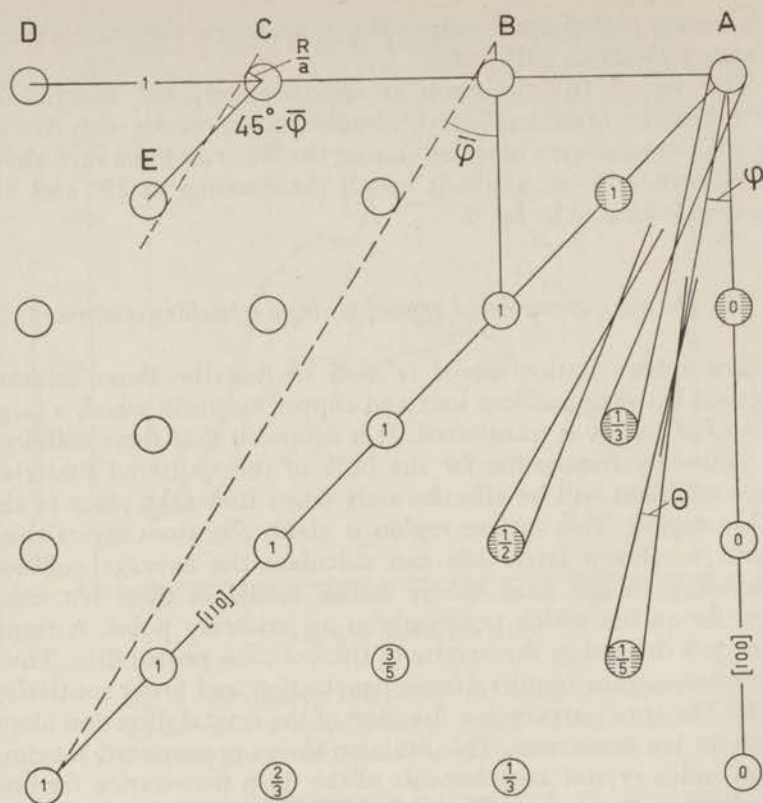
15
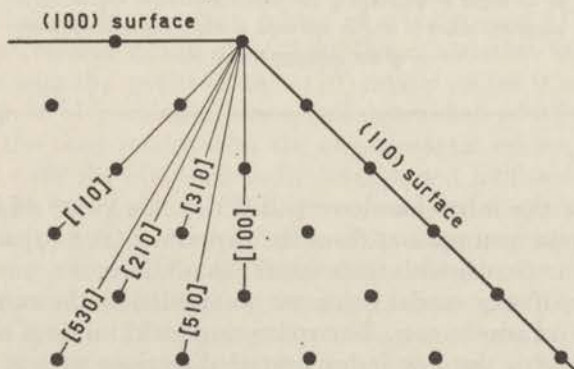
Fig. 6. *An (001) plane perpendicular to the (100) surface of a copper crystal model. The circles represent the effective collision cross-sections for 20 keV Ar⁺ ions colliding with the atoms of the copper lattice. The upper layer represents the surface (A, B, C, D). φ and Θ are denoted for the (510) axis. The partially shaded circles denote the directions, with respect to atom A, in which sputtering minima have been found. The dotted line along atom B shows the direction corresponding to an angle of incidence φ̄ for which maximum sputtering is assumed. Atom C and E are used to show the determination of the collision radius R.*

tential. On the other hand we will derive the value of the radius under certain assumptions from the experimental $S(\varphi)$ curves and compare the results with theoretical calculations.

This transparency model can now be applied to the results of the sputtering measurements. The sputtering yield minima correspond quite well with the low index crystal directions as was shown in

16

section 3. These low index crystal directions are directions with relatively high transparency, mentioned above.

The total angular interval for a minimum in the curve corresponds with the angular interval in which two neighbouring lattice atoms in the low index crystal direction are partially behind each other. The effective collision cross-sections can now be calculated from the width of such an angular interval. In fig. 6 these angular intervals are shown (Θ) for some measured minima. We use the [110] minimum to calculate the radius R for the effective collision cross-section for 20 keV Ar$^+$ and Cu. R is the radius of the hard spheres of our transparency model when the projectile is taken as a point mass. The dotted lines in fig. 6 correspond with a direction for which the atoms nearest to the surface just do not screen each other for the impinging ions. This is the direction in which the maximum sputtering is supposed to occur. The radius R is now determined relative to the distance CE in fig. 6.

$$R = \tfrac{1}{4} a\sqrt{2} \sin (45° - \bar{\varphi}),$$

in which $a = 3.605$ Å, the lattice constant in copper and $\bar{\varphi}$ the angle at which maximum sputtering occurs, being 29° (fig. 2).

A difficulty is the phenomenon that the [110] minimum occurs at 42° instead of 45°, which may be caused by the surface relief of the crystal due to repeated bombardments. Instead of $(45° - \bar{\varphi})$ we use the angle between the directions where maximum and minimum sputtering is found. Then a possible misorientation cancels out to a high degree. Therefore, this value is thought to be more accurate. The angle between those two directions, $\Delta \varphi$, is 13° (fig. 2), from which follows:

$$R = \tfrac{1}{4} a\sqrt{2} \sin 13° = 0.080\, a = \underline{0.29 \text{ Å.}}$$

The angle for the minimum respectively maximum value of the sputtering ratio is determined with an accuracy in the order of 1° corresponding with an accuracy of about 10% in R.

The same calculation for Ne$^+$, where $\Delta \varphi$ is between 11° and 12°, results in a collision radius of $\underline{0.25 \text{ Å.}}$ The calculation for Kr$^+$ has been made with the results for the $(1\bar{1}0)$ crystal on the 0° minimum, where $\Delta \varphi = 11°$, which means a collision radius of $\underline{0.24 \text{ Å.}}$

To check the used model with the experimental curves, we have calculated with the obtained radii the expected half widths of the other minima (see Table I). The agreement is satisfactory when we take into account that most of the minima are overlapping each other to some extent. The widths of the minima in directions with higher indices are smaller than the angular spread of the used ion beam. This means that the angular resolution of our experimental set up is not good enough to detect those minima.

17

TABLE I. Expected half widths of minima.

	crystal direction					
	[100]	[510]	[310]	[210]	[530]	[110]
$\Delta \varphi$, Ne ($R = 0.25$ Å)	8°	3.1°	5°	3.6°	2.7°	11.3°
$\Delta \varphi$, Ar ($R = 0.29$ Å)	9.2°	3.6°	5.8°	4.1°	3.1°	13.1°
$\Delta \varphi$, Kr ($R = 0.24$ Å)	7.6°	3°	4.8°	3.4°	2.6°	10.8°

On the other hand, by using a perfect parallel beam, the number of detectable minima will not increase very much due to the finite size of the lattice atoms.

It is also possible to make a comparison between two maximum values of the sputtering ratio respectively in the Ar case of fig. 2 and that of fig. 3. In the case of fig. 3 a maximum sputtering ratio must be expected at about 28° (from the effective cross-section of 0.25 Å). This is quite well possible taking into account the relative small number of data and the slopes of the sputtering curve in fig. 3 around the minimum in the [2$\bar{1}$1] direction. A maximum sputtering ratio of at least 11 should be expected at 28°. This is higher than the maximum at 29° in fig. 2, which is in qualitative correspondence with the transparency idea, for in both directions of maximum sputtering the crystal model shows opaque planes. From a crystal model one can see that the mutual distance of the (011) planes for the measurements in fig. 3 is smaller than this distance for the (001) planes for fig. 2.

We can also compare the sputtering ratios at 29° and 42° for the Ar case in fig. 2. The 29° direction was connected with that direction in which the hard spheres of our transparency model, when seen in perspective, are just touching when we look along the ion
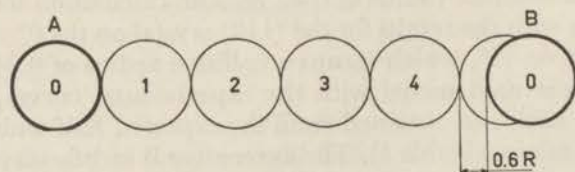

Fig. 7. A [110] atom row projected on a plane perpendicular to the dashed line in fig. 6. Thickly-lined circles represent surface atoms. The numbers in the circles indicate the layer depth under the surface layer in which the corresponding atoms are situated.

direction. This corresponds to the situation shown in fig. 7, where the hard spheres of fig. 6 which are denoted by an index 1, are projected on a plane perpendicular to the dotted line of fig. 6. If we look along a [110] direction we see only the first atoms of the [110] rows.

The distance of these rows is $\frac{1}{2}a\sqrt{2}$. From these considerations follows a transparency ratio $2 \ R \ : \ \frac{1}{2}a\sqrt{2}$ for the 29° and 42° directions of fig. 2, neglecting a minor part of the surface of the atom partially seen in fig. 7. The inverse of this ratio in the case of Ar on Cu is 4.3, which is in reasonable agreement with the ratio of the sputtering yields, being 9.5 : 2.5.

From this proportionality we see that apparently the contribution of the fifth atom layer to the overall sputtering is the same as the first layer does. The decrease of the sputtering yield for incidence angles above 29° to the minimum at 42° in the Ar case cannot be described by the transparency model. We believe that it is necessary to take into account the different directions in which the collision partners can fly away. At incidence angles above 29° the crystal atoms are partially behind each other and consequently the collision partners cannot be scattered in certain directions with respect to the surface.

Fig. 6 shows that it is indeed reasonable to use a crystal model of about ten atom layers to explain the results. Firstly the detection of the [510] minimum means that ion collisions in the sixth layer are still important. On the other hand the chance of first ion collisions for a 20 keV Ar^+ ion on Cu at a depth below 10 atom layers will be small, at any rate in the plane used in fig. 6.

We conclude that the transparency as defined here is useful for a discussion of the qualitative behaviour of the sputtering ratio in our energy region. Nevertheless, it is impossible to describe the moderate slopes of the $S(\varphi)$ curves around the deep minima by the transparency model. A quantitative analytical treatment of the collision possibilities which must be capable of calculating relative sputtering ratios should not disregard the successive collisions.

5. *Discussion*

The collision radii calculated by us in section 4 using a hard sphere approximation are 0.25 Å, 0.29 Å and 0.24 Å for 20 keV Ne^+, Ar^+ and Kr^+ ions on Cu. We will use the name effective radii for these values. Using a Bohr potential for the calculation of collision radii in a hard sphere approximation gives respectively 0.12 Å, 0.17 Å and 0.23 Å for the 20 keV ions on Cu. These Bohr radii are increasing with the mass of the projectiles, whereas the effective radii for sputtering are almost independent of the mass of the projectile. The

ratios of effective radii to Bohr radii are for Ne, Ar and Kr respectively 2.1, 1.7 and 1.0. This discrepancy in systematic behaviour may have the following reason. The calculation of the effective radii is based on projectile movement along straight lines. We can calculate the minimum impact parameter for which this assumption is valid with the help of a Bohr potential (no hard sphere approximation). We assume that an angular deviation of $3°$ in the orbit of the projectile during passage of a lattice atom is negligible. Such an angular deviation is of the order of the angular spread of the ion beam. The impact parameters for which the scattering angle is only $3°$ are 0.43, 0.47 and 0.51 Å for Ne, Ar and Kr on Cu respectively. Therefore, we may indeed expect that the yield curves for Ne, Ar and Kr on copper have about the same structure. Such a scattering angle of $3°$ in the laboratory system corresponds to energy transfers of 17 eV, 37 eV and 72 eV for Ne, Ar and Kr respectively, which is not much above the displacement energy in copper.

To get an idea about the energy transfers involved, we calculated the energy transfer, using a Bohr potential, for collision parameters corresponding to the values of the effective radii[14]). The scattering angles in the center of mass system are respectively $17°$, $18°$ and $50°$ for Ne, Ar and Kr on Cu, corresponding to transferred energies of 300 eV, 450 eV and 3500 eV and scattering angles in the laboratory system of $13°$, $11°$ and $21°$ respectively. This is much more than we may accept for our model. We should expect to find the effective radii closer to those calculated for a $3°$ deviation of the original direction. This discrepancy is not yet understood.

It may be doubtful to which extent we may use fig. 6 as an average over different planes through the atoms of the lattice. A projectile penetrating in a (001) plane somewhat shifted from that through the copper nuclei is bent somewhat out of that plane. This means that these planes are becoming less important for the description of mutual screening of lattice atoms.

Channeling may have an influence in the $S(\varphi)$ curves. It is possible that the region of the cross-section of an atom where the scattering angles are such that the projectiles are bent into a [110] channel is dependent on the direction in which a certain crystal is bombarded. The total extra chance of channeling (besides these open directions which are already taken into account in our model) will, nevertheless, be relatively small.

Focusing ejection mechanism will not be important in a treatment which is used for relative values of sputtering ratios. A large number of collisions is necessary to reach mean energies as low as required for internal focusing. The direction of the knocked on particles will on the average have no relation to the original direction of the ion after a number of collisions. This means that the probability of

focusing does not change with the crystal orientation along which an energetic ion penetrates.

As yet we have not discussed the possible influence of lattice vibrations and noble gas content on the calculated radii or on the penetration depth. The noble gas content can increase the mean density and give higher sputtering ratios, especially in the most open directions, where Almén and Bruce[3] measured a very high noble gas content. However, since only the first surface layers are very important to sputtering and the greater part of the noble gas content will be much deeper in these open directions, the influence of the gas on the sputtering yield should be small at room temperature[13]. Lattice vibrations are slow compared to the velocity of the projectiles. This means that the most dense lattice structure for the projectile is somewhat more open but it remains, as a mean, the most dense one. The angles at which minima and maxima occur are not changed, however, they will be not as sharply defined as those which would be expected from a static gas-free lattice.

REFERENCES

1. Rol, P. K., Fluit, J. M. and Kistemaker, J., Physica **26** (1960) 1009.
2. Bohr, N., Kgl. Danske Videnskab Selskab, Biol. Medd. **18**, no. 8, 1948.
3. Almén, O. and Bruce, G., Nucl. Instr. and Meth. **11** (1961) 257.
4. Fetz, H., Z. Physik **119** (1942) 590.
5. Rol, P. K., Fluit, J. M. and Kistemaker, J., Physica **26** (1960) 1000.
6. Wehner, G. K., J. Appl. Phys. **30** (1959) 1762.
7. Wehner, G. K., Phys. Rev. **102** (1956) 690.
8. Koedam, M., Physica **25** (1959) 742 and thesis, Universiteit Utrecht (1961).
9. Rol, P. K., Fluit, J. M., Viehböck, F. P. and de Jong, M., Proceedings of the IVth international conference on ionization phenomena in gases, North Holland Publ. Cy., Amsterdam (1960) 257.
10. Ogilvie, G. J., J. Phys. Chem. Solids **10** (1959) 222.
11. Laponsky, A. B. and Rey Whetten, N., Phys. Rev. Letters **3** (1959) 510.
12. Dekker, A. J., Phys. Rev. Letters **4** (1960) 55.
13. Fluit, J. M., Snoek, C. and Kistemaker, J., to be published in Physica.
14. Everhart, E., Stone, G. and Carbone, R. J., Phys. Rev. **99** (1955) 1287.

SURFACE STRUCTURE OF IONICALLY BOMBARDED
COPPER SINGLE CRYSTALS

---

1. *Introduction*

It has been long known that when a metal is sputtered by ion bombardment the resulting surface displays rather regular geometric features[1,2]). Since, in the case of polycrystalline materials, the grain boundaries are selectively attacked, ion bombardment techniques have been developed for use in metalographic studies. Early workers in this field had noted that the surface structure was a function of the ion energy and target temperature. More recent investigations have demonstrated a strong dependence upon the ion beam incidence angle[3]).

In work previously reported (see also chapter I), a study was made of the dependence of the sputtering yield of copper single crystals as a function of the incidence angle of a 20 keV noble gas ion beam with respect to a fixed crystalographic orientation[4]). In this work it was observed that repeated measurements made in the same experimental configuration were reproducible to within 3 % but if measurements were made at other incidence angles before returning to the original angle the reproducibility was only 10 %. This "memory" effect was attributed to the change in the microstructure of the surface with changing incidence angle and was the motivation for the present work.

2. *Experimental conditions*

A copper single crystal, which was cut along a (100) plane, was afixed to a rotatable holder and mounted in the collector chamber of a 180° isotope separator. The crystal surface was *ca* 3 × 2 cm² in area and a shutter system was arranged such that separate spots on the crystal surface (*ca* 5 mm in diameter) could be exposed to the beam. The crystal could be rotated about a [100] direction in

the surface plane and a given spot bombarded so that the effect of incidence angle could be studied on a single surface. The temperature of the sample was maintained at *ca* 40°C by cooling with liquid ether during bombardment. The isotope separator furnished a beam of 20 keV Ar^+ ions with a current density of 500 μ A/cm^2 and an angular divergence of 3°. Since, at this current, the rate at which surface atoms are removed by sputtering (*ca* 10^{16} atoms/cm^2 s) far exceeds the flux of incoming oxygen molecules from the ambient gas (partial pressure of *ca* 1×10^{-6} torr), the surface was almost certainly free of oxide contaminants.

3. *Results*

Optical microscopic examinations of the surface following bombardment revealed highly regular surface structures typified in Figs. 1 and 2.

The texture in Fig. 1 is obtained by bombardment at normal incidence while the ridge-like structure in Fig. 2 is obtained at 45° incidence. The depths of the irregularities in all cases were in the order of 1 μm. This depth was attained after the removal of *ca* 10 μm

Fig. 1. *Microphotograph of the surface of a (100) copper crystal which has been bombarded by 20 keV Ar+ ions at normal incidence.*
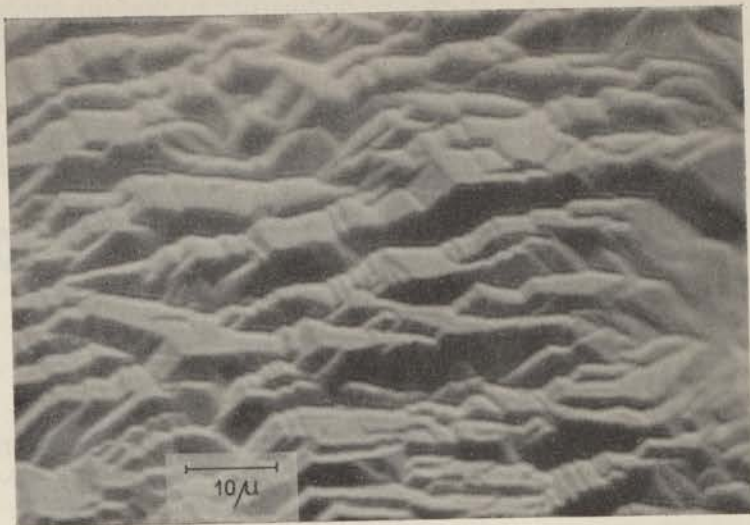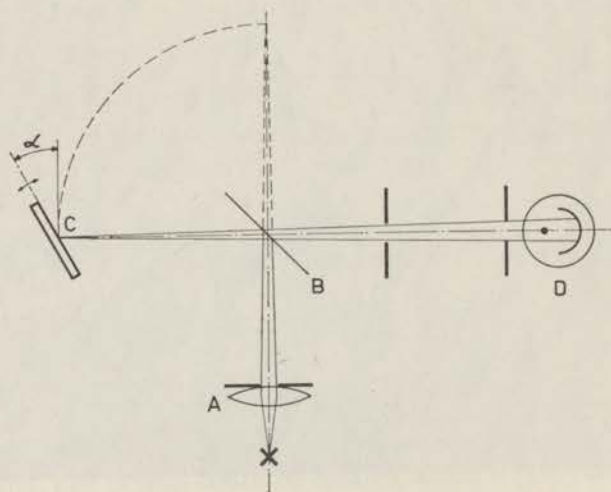
Fig. 2. Microphotograph of the surface of a (100) copper crystal which has been bombarded by 20 keV Ar+ ions at 45° to the normal, i.e. in a [110] direction.

Fig. 3. Schematic diagram of the apparatus used for the light reflection measurements.

of material from the surface by sputtering. Upon further sputtering, the pattern and magnitude of the surface, irregularities remained substantially the same, but the surface projections were not necessarily the same ones that had been observed previously.

In order to determine the overall orientation of the surface ridges, light reflection measurements were made with the apparatus pictured in Fig. 3.

The lightbeam was focused by the lens A to converge at point C on the copper surface after being reflected from a half silvered mirror at point B. Part of the light reflected at 180° to the incoming beam passed through the half silvered mirror and was measured by the photocell D. The angular aperture of the optical system was $\approx 2°$. The single crystal was rotated through the angle α about the same [100] direction which defined the ion beam incidence angle φ. The results of the light reflection measurements as a function of α are shown in Fig. 4 for the four different ion bombardment angles.

The measurements plotted in Fig. 4 were made on target areas from which the amount of copper removed corresponded to an average depth of 40, 80, 20 and 40 microns for Fig. 4A, 4B, 4C and 4D respectively. Patterns obtained from samples which had been bombarded for only half this time were quite similar.

Except for the case of normal incidence, rotation of the crystal about an axis in the crystal surface plane perpendicular to the one defining α, indicated random reflection planes (cosine distribution).

4. *Discussion*

First let us consider the patterns obtained with 30° and 37.5° (Fig. 4C and 4D). In this case the predominant ammount of sputtering is due to focused collision sequences emmanating from centers of energy degradation which lie just below the surface. Since the density of these centers is proportional to the flux, and the flux at the surface is dependent on the incidence angle, it would be expected that surface facets perpendicular to the incidence angle would tend to be developed. The picture, however, is not quite this simple, since the focused collision sequences responsible for the removal of surface atoms are not randomly directed, but instead are propagated in close-packed crystal directions. For the case of the face-centered cubic structure they are the [110] directions and, to a lesser extent, the [100] directions. It would, therefore, be expected that the surface planes, developed by the focusing mechanism, would be intercepted by a maximum number of these axes since there is a higher probability for atom removal in these directions. Thus, for a crystal originally with a (100) surface which has four [110] directions leaving this surface, one might expect the develop-

25

ment of (110) planes having an angle of 45° with the original surface, since these planes have five [110] directions emerging from the surface.

The combinations of these two effects is seen in the left hand portions of Fig. 4C and 4D. In the case of the 30° bombardment a strong reflection peak appears at $\alpha = 40°$ which lies between the close-packed (110) plane at —45° and the normal incidence plane at — 30° (α is taken negative in the left quadrants of Fig. 4). For 37.5° incidence (Fig. 4D) the strong reflection peak is almost per-

Fig. 4. Polar plots of the α-angular dependence of the intensity of the light reflected from a (100) copper monocrystal surface which has been bombarded by 20 keV Ar^+ ions at the given angles of incidence φ. Since the ion beam direction was turned in a (100) plane the angles 45° and — 45° correspond to [110] directions as shown in D. The dotted circle shown in D corresponds to the light distribution which would be obtained from a diffuse reflector.
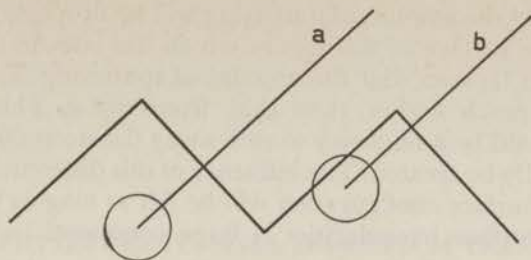

(A)   0° ion incidence

(B)   45° ion incidence

(C)   30° ion incidence

(D)   37,5° ion incidence
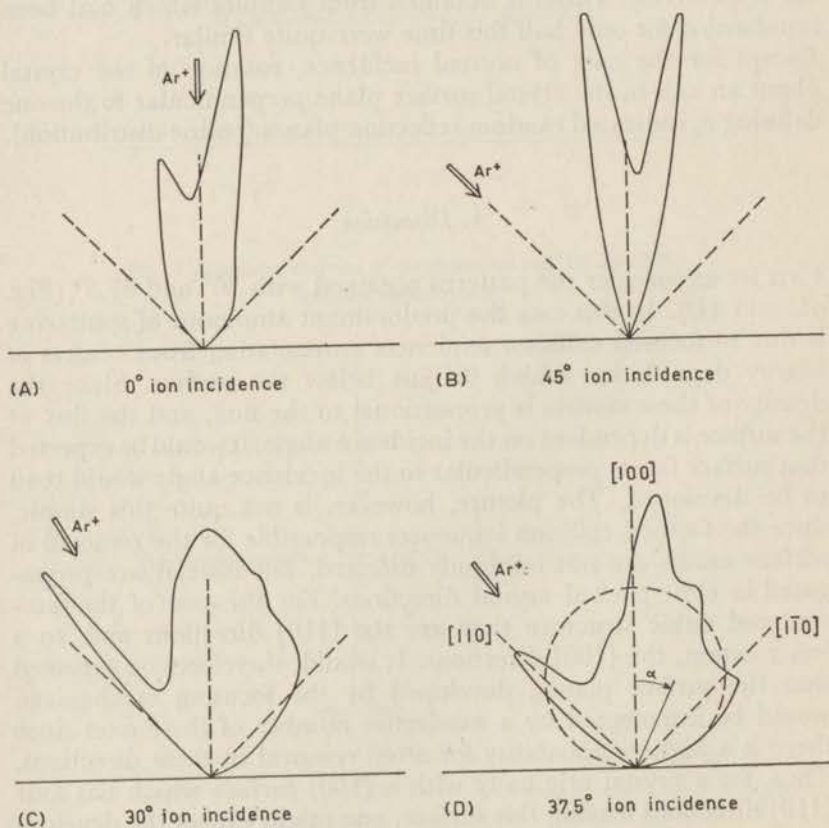
Fig. 5. Schematic diagram showing the influence of ion penetration depth on the differential etching of surface irregularities.

fectly coincident with the [110] direction at —45°. Although the remainder of the pattern is highly diffuse the development of the other low index planes, (100) at 0° and (110) at +45°, is also evident.

The same combination of mechanisms might be used to explain the pattern obtained for normal ion incidence (Fig. 4A). Here, two reflection peaks appear which lie between the directions favoured by maximizing the flux (0°) and the close-packed [110] directions (45°). The lack of complete symmetry here must be attributed to an asymmetry in the divergence of the beam striking the surface.

The only pattern which is inexplicable with only the above set of mechanisms was that obtained at 45° incidence (Fig. 4B). Here it would be expected that one would obtain sharp peaks at 45° to the surface normal since, in this case, both the maximized flux and close-packed direction requirements are coincident. This peak, however, did not in fact materialize but instead only irregularities having a very small angle (*ca* 15°) with the original surface were developed. In order to understand this phenomenon we must recall the results of the previously reported work on the dependence of the sputtering yield upon incidence angle[4]). In this work, it was shown that sharp minima existed in the sputtering yield when the beam entered in low index ([110] and [100]) directions. These minima were explained on the basis of a high probability for deep penetration of the ion into the crystal lattice before making a primary ("hard") collision with a lattice atom.

The effect of this high penetration probability at 45° incidence would be to minimize the angle of the facets with respect to the surface. This may be seen in Fig. 5.

Here, we shall consider the effect of ion penetration depth on a hypothetical crystal surface which has developed 45° ridges. In Fig. 5 we have depicted the situation where the penetration depth is high compared to the radius of the energy degradation sphere. If

27

we assume that the amount of sputtering will be proportional to the fraction of the surface of this sphere which lies outside the crystal surface, it can be seen that the amount of sputtering due to ray *b* will be very much higher than that from ray *a*. Thus, in this case there would be a tendency to etch away the steep slopes which would normally be created. The influence of this differential etching effect on the surface configuration will be felt as long as the amplitude of the surface irregularities is large compared to the penetration depth.

REFERENCES

1. Wehner, G. K., "Sputtering by Ion Bombardment" in "Advances in Electronics and Electron Physics", L. Marton, editor (Academic Press, Inc., New York, 1955), Vol. VII.
2. Numerous recent articles relating to these phenomena may be found in "Le Bombardement Ionique" (Editions du Centre National de la Recherche Scientifique, Paris, 1962).
3. Haymann, P. and Waldenburger, C., ibid p. 205.
4. Fluit, J. M., Rol, P. K. and Kistemaker, J., J. Appl. Phys. **34**, 690 (1963).

SPUTTERING BY SMALL MOMENTUM TRANSFERS
OF 20 keV IONS TO SURFACE ATOMS

1. *Introduction*

It is now reasonably well established that the mechanism primarily responsible for sputtering of metals by high energy ions[1,2]) is that due to focused collision sequences, which follow the collisional degradation of the ion's energy below the surface of the metals. Another mechanism which could also contribute to sputtering is the direct transfer of momentum from an incoming particle to a surface atom, while entering the crystal. In this chapter we shall consider the contribution of this effect to the sputtering of Cu by 20 keV Ar$^+$ ions. An estimate of the magnitude of this contribution can be obtained by calculating the probability of an Ar$^+$ ion ejecting a Cu atom from the surface.

The minimum energy transfer necessary for sputtering is about 5 eV (vaporization energy). The maximum energy transfer can be chosen equal to 10 eV, being the sum of the vaporization energy for a copper atom and an accepted higher value of the sputtered atoms (5 eV), taken from Wehners recent result[3]). In this energy range of 5—10 eV the effective cross-section for sputtering by direct momentum transfer should be quite large. The cross-section can be estimated by calculating the impact parameter necessary for this amount of energy transfer from the scattering potential applicable in this range. If one assumes that the scattering potential, $V(r)$, measured for Ar on Ar by Amdur and Mason[4]) for the energy region 0.2 to 1.3 eV, is approximately valid for 5—10 eV energy transfer from Ar to Cu, the effective radii, r, can be found from the relation:

$$V(r) = 840 \times r^{-8.33},$$

where $V(r)$ is the potential in eV. This yields an effective radius from 1.7 to 1.9 Å. A consideration of the geometry of the copper
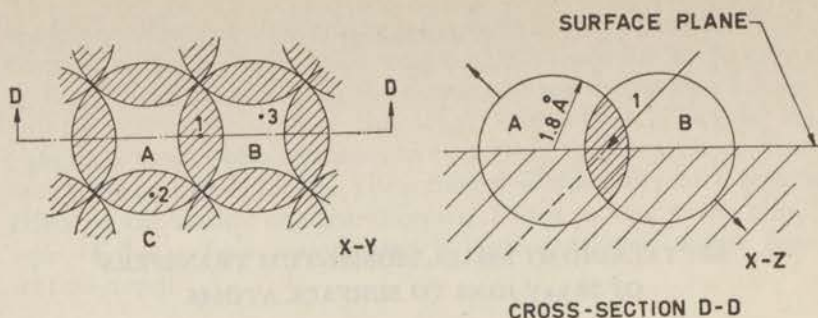
Fig. 1. *The surface of a copper crystal in which the diameters of the Cu atoms represent the effective size for transfer of > 5—10 eV from an incoming 20 keV Ar$^+$ ion. The shaded areas represent the area of overlap between the spheres. An Ar$^+$ ion in the X–Z plane entering at 45° to the X–Y plane, and striking it at point 1, will eject atom A and drive atom B into the crystal (S = 1). An ion entering somewhat to the right side of point 2 will eject both atom A and atom C depending on the direction of incidence (S = 2), while an ion entering at point 3 will only drive atom B into the lattice (S = 0). Integration of all possibilities gives a sputtering yield of ≈ 1 for this mechanism.*

lattice, in which the nearest neighbour distance is 2.5 Å indicated that the entering Ar$^+$ ion must impart at least this energy to at least one copper atom (see fig. 1). The direction into which the Cu atom will be scattered will depend upon the energy transferred, but — because the cross-section decreases with increasing energy transfer — most of the scattering will involve small energy transfer, and will take place in a region close to 90° with respect to the incident ion direction. (In these collisions the direction of the fast Ar$^+$ ion is almost unperturbed.) For oblique ion incidence, the momentum imparted by one half of these collisions will be directed outward from the surface and should give rise to sputtering. At 45° the sputtering yield S, should be about 1 as explained in the legend of fig. 1.

Although the sputtering yield of 20 keV Ar$^+$ on polycrystalline Cu is *ca* 8, it has recently been shown that the total sputtering yield for ion incidence along the [110] and [100] directions is only 3.[5]) Thus, in this case the contribution of this process to the total could become important.

2. *Experiment*

In order to verify the above assumption, the following experiment was performed. A (100) copper single crystal was placed in an electromagnetic isotope separator and bombarded by a 20 keV Ar+ ion beam along a [110] axis (45° incidence), as shown in fig. 2. Six glass collecting plates were placed in the indicated positions and the amount of copper sputtered onto them was determined by weighing. In an experiment in which the crystal was bombarded by an inte-

---

Fig. 2. The experimental set-up for the determination of asymmetric sputtering. A 20 keV Ar+ ion beam is injected along X—O on a (100) copper single crystal. O—X and O—Y are [110] directions of the single crystal which means that the centers of focused spots were at X and Y. The sputtering in a plane O A A' perpendicular to O—X was compared with sputtering in backward directions in plane O B B'. This was done by comparing the amount of copper collected on plate 3 and plate 6 with that on plate 1 and plate 2. O—X = O—Y = 98 mm; plate dimensions: 6 × 42 mm².
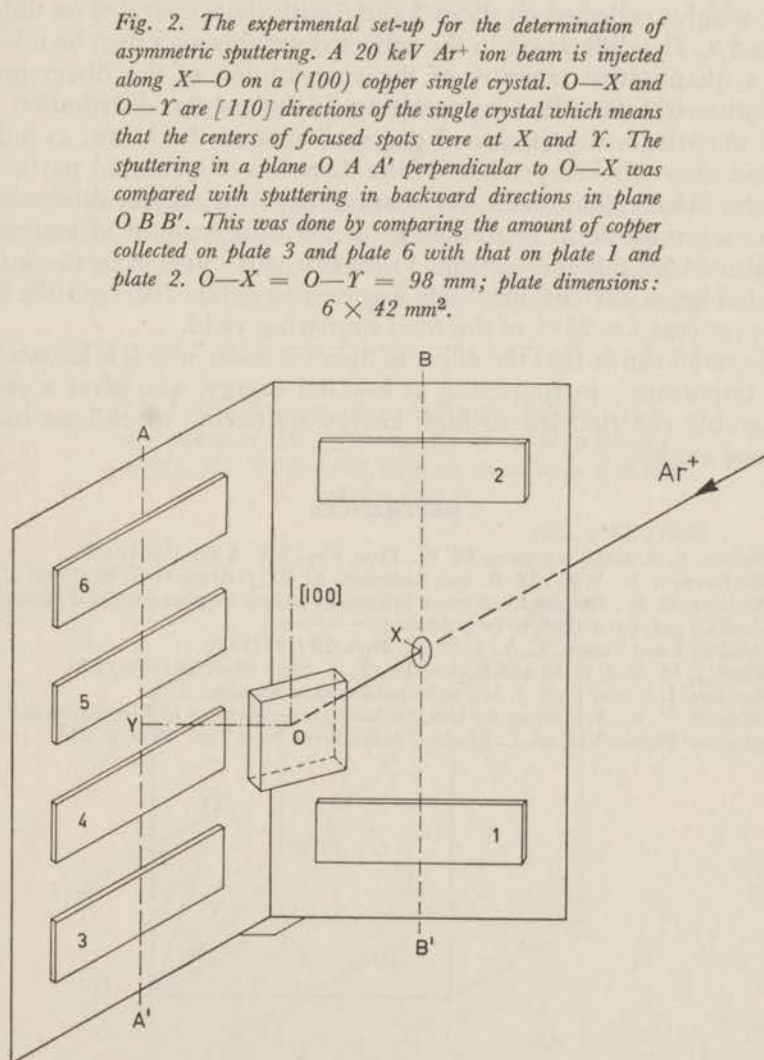
grated current of 3 coulombs, the weights of copper found on the plates 1—6 were: 58, 55, 88, 119, 127, 92 μg, respectively. Since the glass slides were placed symmetrically around the position of the well-known [110] focused collision spots, one would expect the contribution of focused[1]) and crowdion[6]) sputtering to be symmetrically distributed, close to the center of these spots. The fact that the maximum weights were obtained on slides 4 and 5, is in accordance with this expectation.

The bulk of the material sputtered by direct momentum transfer, should be equally distributed in the plane OAA' (see figure 2), perpendicular to the direction of the incoming beam. The direct momentum transfer effect may, therefore, be seen by comparing the weights collected on slides 3 and 6 with those collected on slides 1 and 2. The differences in the collected weights may then be taken as a quantitative measure of the contribution of the direct momentum transfer effect to sputtering. If the angular distribution of the material which is ejected perpendicular to the beam, as indicated above, is independent of the direction of sputtered particles in the OAA' plane, then the integration of the weight differences over a semicircle in this plane gives the total amount of material sputtered by this mechanism. From this value and from the integrated beam current, one finds a sputtering ratio of $0.7 \pm 10\%$ for this process, i.e. 25% of the total sputtering yield.

The result shows that the effect of direct transfer which is known to be important[7]) in sputtering at low ion energy, also gives a considerable contribution to high energy sputtering at oblique incidence angles.

REFERENCES

1. Nelson, R. S. and Thompson, M. W., Proc. Roy. Soc. A **259** (1961) 458.
2. Southern, A. L., Willis, W. R. and Robinson, M. T., J. Appl. Phys. **34** (1963) 153.
3. Wehner, G. K., Sixième Conférence Internationale sur les phenomènes d'ionisation dans les gaz, Paris 1963, to be published.
4. Amdur, I and Mason, E. A., J. Chem. Phys. **22** (1954) 670.
5. Fluit, J. M., Rol, P. K. and Kistemaker, J., J. Appl. Phys. **34** (1963) 690.
6. Sanders, J. B. and Fluit, J. M., to be published in Physica.
7. Wehner, G. K., Sputtering by Ion Bombardment. Advances in Electronics and Electron Physics VII, ed. L. Marton, Acad. Press, New York, 1955, p. 239.

## SPUTTERING OF COPPER BY ION BOMBARDMENT AT TARGET TEMPERATURES BETWEEN 40° AND 900°K

1. *The influence of target temperature on focused collisions and its consequence for sputtering*

The focused collision sequences along the close-packed crystal axes, mentioned in the Introduction, transfer momentum from one atom to its neighbour. In such collision chains the momentum is exactly in the direction of that axis after 4 or 5 collisions. The range of such

Fig. 1. Atom O moving along a close-packed direction collides at P with atom (101) after an energy loss due to the particles at 011, 011, 110 and 110, all at the same distance from the collision point P.
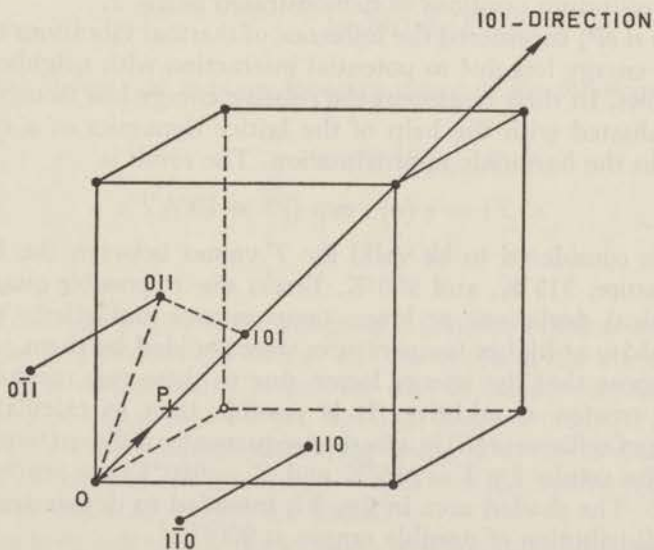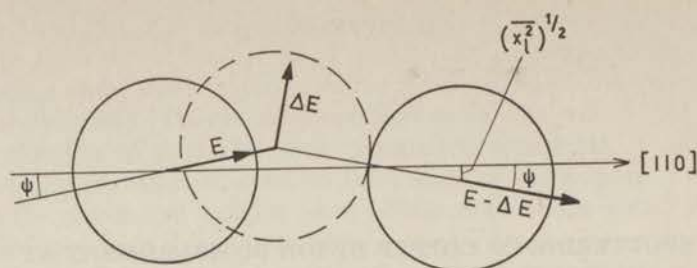
Fig. 2. Scattering effect and kinetic energy loss by thermal vibrations of atoms belonging to a [110] axis. The mean square deviation from equilibrium position normal to the [110] axis is denoted in the fig. by $(\overline{x_1^2})^{\frac{1}{2}}$.

a focusing sequence has been calculated by Leibfried[11]) for a static copper lattice, using a Born-Mayer potential. For the colliding atoms a hard sphere model is used. This range is determined from the energy lost at every collision in the sequence by potential inter-action with the four neighbouring [110] rows (cf. fig. 1).

The maximum recoil energy for which focusing is possible, E_f, is 63 eV, in this treatment. The relative energy loss per collision, as calculated by Leibfried, is then $\varepsilon\,(\mathrm{o}) = \Delta\,E/E = 1.1 \times 10^{-2}$, from which would follow a range of about 250 Å.

This treatment has been extended to a vibrating lattice in two different ways. Nelson et al[3]) took into account the loss of kinetic energy per collision due to the displacements of the colliding atoms from equilibrium positions as demonstrated in fig. 2.

Sanders et al[4]) considered the influence of thermal vibrations on the relative energy loss due to potential interaction with neighbouring [110] rows. In their treatment the relative energy loss factor $\varepsilon\,(T)$ was evaluated with the help of the lattice dynamics of a copper crystal in the harmonic approximation. The result is

$$\varepsilon\,(T) = \varepsilon\,(\mathrm{o}) \cdot \exp\,(23 \times 10^{-4}\,T),$$

which is considered to be valid for T values between the Debye temperature, 315°K, and 900°K. Errors due to possible quantum-mechanical deviations at lower temperatures and effects of an-harmonicity at higher temperatures were avoided by them.

We propose that the energy losses, due to these two mechanisms can be treated as additive. It is possible then to calculate the number of collisions $n(E)$ in a focused sequence for different temperat-ures. The results for $T = 315°K$ and $T = 900°K$ are represented in fig. 3. The shaded area in fig. 3 is intended to demonstrate the broad distribution of possible ranges at 900°K.

34

The calculated ranges of [110] focusing collision sequences can be used for an interpretation of the total sputtering ratio as a function of target temperature. The average range, for a given temperature, can be calculated if we know the probability $W(E)$ for a focusing collision to start at some energy E below E_f. $W(E)$ is taken proportional to the solid angle in which focusing is possible for a specified [110] direction. This means that we assume that the recoil particles, before participating in a focused collision, are moving in a random way through the lattice. This assumption is allowed for "high energy sputtering" because of the large number of collisions necessary to reach energy values in the order of E_f, from which follows that no appreciable memory of the initial ion direction is expected.

The focusing solid angle is $2\pi \ (1 - \cos \vartheta_F)$, where ϑ_F is the maximum angular deviation from the [110] axis for which focusing is possible at the energy $E < E_f$.

$$W(E) = \frac{2\pi \ (1 - \cos \vartheta_F)}{2\pi} = 1 - \frac{D}{2R \ (E)}$$

The second equality has been taken from ref. 11. $R(E)$ is the hard sphere collision radius and $D \ (= 2.55 \ \text{Å})$ is the closest distance between copper atoms in their lattice. When $R(E)$ is calculated from

$E = 2A \exp\left(-\frac{R}{a}\right)$ with $A = 21$ keV and $a = D/13$, then $R(E) = \frac{D}{13} \ln \left(\frac{2A}{E}\right)$. Using $E_f = 63$ eV we get $R(E) = D/13 \ln \ (667 \ E_f/E)$ from which follows

$$W(E) = 1 - \frac{6.5}{\ln \ (667 \ E_f/E)}.$$

We now define an average focusing range in the following way:

$$\overline{n(E)} = \frac{\int\limits_{E_b}^{E'_f} n' \ (E) \ W(E) \ \mathrm{d}E}{\int\limits_{E_b}^{E'_f} W(E) \ \mathrm{d}E}$$

In this formula $n' \ (E)$ is the range of a focused collision sequence up to the point where the energy has decreased to E_b, the binding energy of a surface atom, which for ease of calculation has been chosen to be equal to 5 eV (cf. fig. 3 at $E/E_f = 0.08$). E'_f is the maximum focusing energy according to fig. 3. $n' \ (E)$ is calculated from fig. 3 with the relation $n' \ (E) = n(E) - n(E_b)$, where $n(E_b) \approx 3$ for 315°K and $n(E_b) \approx 0.5$ for 900°K.

$\overline{n(E)}$ has been calculated numerically, and has been found equal to

35

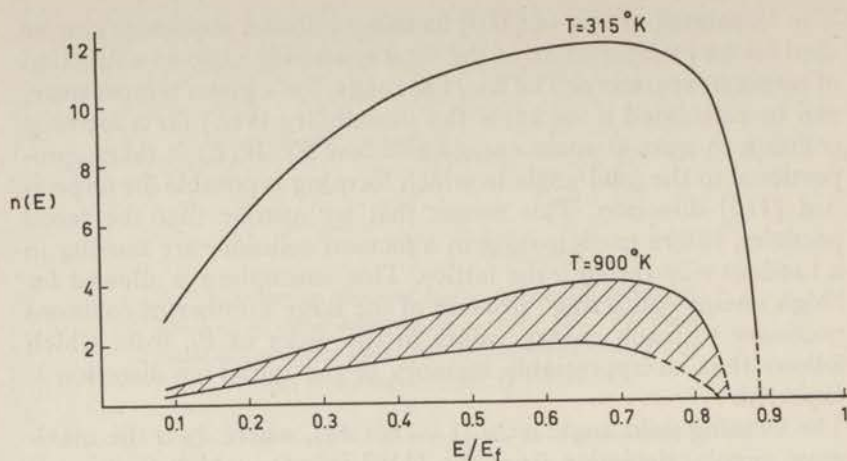*Fig. 3. The number of collisions n(E) in a focused collision sequence in slowing down from energy E, calculated from theory. E/E_f is the energy with which the focusing sequence starts, expressed as the fraction of the maximum focusing energy E_f.*

5 for a copper target at 315°K. This means that we can imagine a "sheath" at the surface, consisting of the first few atom layers to a thickness between $4D$ and $5D$ (depending on the orientations of the [110] axes to the surface plane) through which momenta from recoil atoms inside the metal have to be focused so that the focused sequence is able to eject a surface atom. Using the fact that the majority of the sputtered particles have an energy well below E_f', we conclude that this sheath acts as a highly focusing medium, because through a given lattice site at least four [100] axes are directed toward the surface, which means a focusing probability of at least $4 W(E)$. This total probability is greater than 0.5 for $E_f/E = 0.3$ and increases with E_f/E.

For copper at 900°K the value of $\overline{n(E)} = 2$. The "sheath" is very thin and a recoil particle with $E < E_f'$ has a considerable chance of passing its momentum through, without it being focused.

This description is in accordance with the strong dependence of the size of the [110] spots on temperature as measured by Nelson et al[2]. Moreover, this description shows that the [110] sputtering yield is not proportional to the length of the average range of focusing collision sequences. The defocusing or crowdion collisions[11, 19] also have ranges of this length. Their contribution to sputtering increases with target temperature and compensates for the decrease of the number of atoms ejected by focused collision sequences. This is in accordance with our measurements of sputtering yields from

36

polycrystalline copper by 20 keV noble gas ions for target temperatures between 300°K and 600°K, which gave almost constant values within the accuracy of measurement (about 10%).

2. *Introduction to low target temperature sputtering*

The sputtering ratio of f.c.c. metals has been measured for target temperatures above room temperature. Almén and Bruce[1]) measured, with 45 keV Kr^+ ions, the sputtering yields of Ni, Pt and Ag between 300° and 1100°K. They found for Ag a constant sputtering ratio, S, for target temperatures between 300° and 900°K, whereas Ni and Pt showed a monotonic decrease of S of roughly 30% over this temperature range. Recent measurements with 20 keV Ar^+ ions on copper at 300°—600°K at our laboratory[2]) gave indications for a small increase in the order of 10%. These slow but rather steady changes of S of the order of 0—3% per 50°K over extended temperature ranges are quite different from the changes in S found in the present work for copper targets below room temperature. From theories which describe the temperature dependence of S above the Debye temperature[3,4]) of the metal, one can indeed expect small even changes in S. These theories describe the influence of temperature on the ranges of focusing collision sequences. The average length of the focusing collision sequence diminishes when the amplitude of the lattice vibrations increases, this causing a decrease in the sputtering arising from these focused collisions. Experimental evidence for the influence of focusing collisions on sputtering was given by Nelson and Thompson[5]). The extent to which the direction of the ejected particles is focused towards the [110] directions was measured for Au as a function of temperature. The spots due to particles ejected in [110] directions were markedly more peaked at lower target temperatures.

Fig. 4. *Relative importance of focusing and defocusing collision sequences at different temperature* $(T_1 < T_2)$.
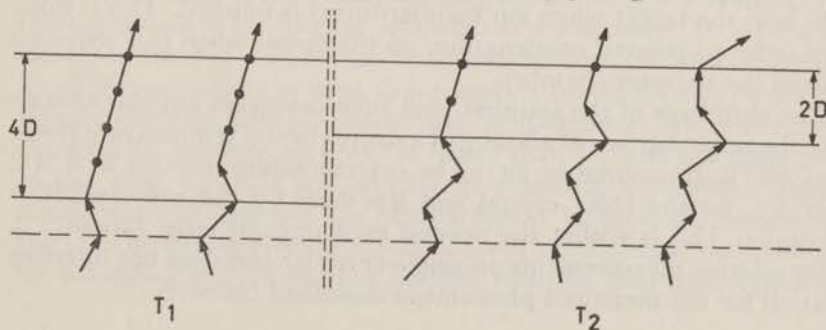
We propose that these focusing events can be distorted by interstitial copper atoms, which will accumulate at low temperatures, and the results of the measurements described in this chapter, are interpreted on this basis. This interpretation cannot be done in a quantitative way, for it is not known to what extent the total sputtering is a consequence of focusing events with a relatively long range. The total contribution of surface sputtering caused by:
1. a large impact parameter collision of the primary ion with lattice atoms of the first surface layers,
2. crowdion movements of recoils in the first surface layers and,
3. focusing events started at two or three layers under the surface, will be independent of temperature as well as independent of the concentration of interstitials and vacancies because of their relative independence of the actual configuration of the lattice atoms.

3. *Experimental arrangement*

The experimental arrangement sketched in fig. 5 shows the target mount and the cooling system as it is arranged at the collector side of an electromagnetic isotope separator.

Polycrystalline targets (surface 2 cm², thickness 2 mm) and single crystals (surface 3 cm², thickness 6 mm) are mounted at A in graphite holders B. The sputtering ratio was determined from weight loss and integrated current measurements as described more extensively before[6]). A diaphragm K at earth potential was used as a screen to prevent ions from reaching the graphite holder. The experiments are performed with 20 keV noble gas ion beams of normal incidence. The actual average incidence angle was found to be 2°—3° off the normal. The sputtering ratio is very sensitive to the angle of incidence when the ions are directed along low order crystal axes as is done here, but the angular spread of the beam diminishes this sensitivity[6]). The target is cooled by contact with the copper plate D, which is soft soldered to the copper tube F, which is cooled by a cooling liquid in the stainless steel "dewar". The copper tube is surrounded by a heating coil E, which is used to heat the target when ion bombardment is finished. This is done in order to prevent condensation on the target when it is removed from the vacuum chamber.

The shrinkage of the stainless steel tube causes an angular change of the target surface of about $\frac{1}{4}$ of a degree over a temperature range of 300°K (measured in air). The corresponding increase in S is 2 or 3% for the (100) crystal and less than 1% for polycrystalline copper. This is within the normal experimental error (about 3% for relative measurements on single crystals) and does not interfere at all for the measured phenomena described below.

38
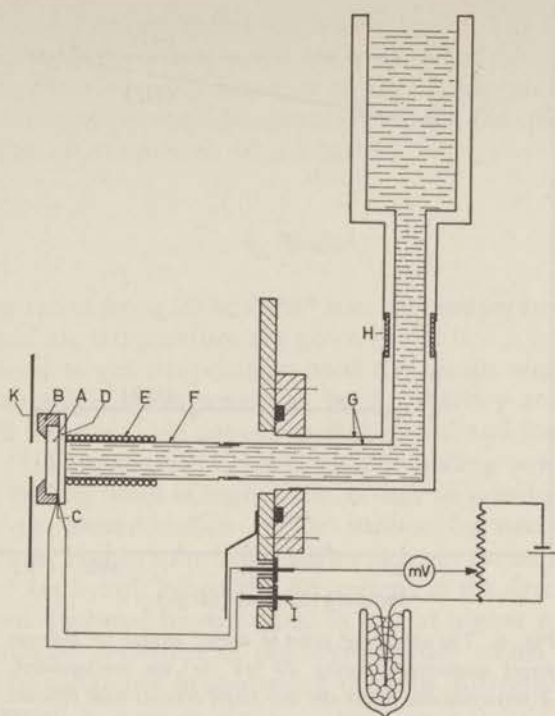
Fig. 5. The target mount at the collector flange of an isotope separator for the determination of sputtering ratios at low temperature.

The insulator H was kept free from condensation with the help of a stream of compressed air. The temperature was measured with an iron-constantan thermo-couple imbedded in the graphite target holder at C, where it was forced through a hole against the target. The thick copper feed-throughs I in glass are screened from possible beam "reflections". The thermo-emf is measured by a compensation method, using a "Bleeker's" comparator, to get rid of the influence of the stray field of the separator magnet on the meter reading. A thermo-couple in melting ice was used as a reference. To facilitate the calculation of an absolute temperature from the observed emf a calibration table was used to interpolate between fixed points at liquid hydrogen, nitrogen and oxygen temperatures. This procedure can give an absolute accuracy of better than 5°, which is sufficient in our case, for it is not possible to maintain a constant target temperature during the ion bombardment because of changes in the ion current. A given temperature was reached and maintained by balancing the ion current heating with the heat leak from the
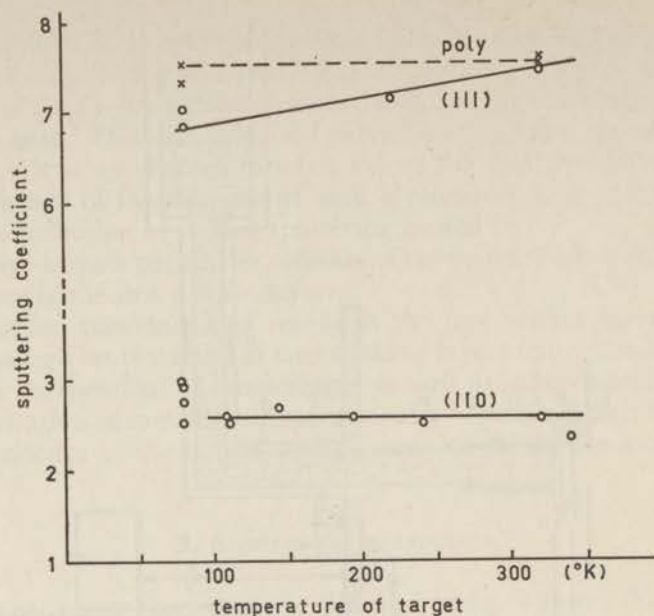
39

Fig. 6. The sputtering ratio of copper targets for different target temperatures during 20 keV Ar⁺ ion bombardment. A polycrystalline target and two single crystals with different orientations of the surface exposed to sputtering were used.

cooling liquid. In this way we were able to maintain a given temperature to within 5°. The surface temperature in the sputtering area will not differ significantly from the target temperature measured in this way, since the lifetime of the thermal spike caused by a single ion is short compared to the average time between the creation of such spikes in a given lattice area. Nevertheless, there may be a systematic error in the stated temperatures of about 7° in the region below 100° K, since the "temperature" measured in the separator without beam was always about 7° higher compared with the "temperature" measured with the thermo-couple in liquid hydrogen. The contact between target A and copper plate D was the same for all measurements. This had to be checked separately by measuring the rate of temperature decrease. A target which is 40° warmer than plate D should cool down by liquid hydrogen at a rate of 2° per second in the first 15 seconds. At low temperatures the chance of condensation and the mean residence time of the condensed state of atoms from the ambient gas in the separator is increased. The possible influence of adsorbed gases on the measured sputtering ratios was checked by diminishing the 20 keV Ne⁺ ion beam current from 100 to 50 μA/cm². For

40

$(100 \pm 25) \mu A$ the same values for S were found, but at 50 $\mu A/cm^2$ the sputtering ratio was lowered by a factor of two. This can be compared to earlier measurements on copper targets at temperatures somewhat above room temperature where, the sputtering ratio remained constant down to 10 $\mu A/cm^2$ [8]).

4. Results

Sputtering ratios from 20 keV Ar^+ ions for temperatures down to about liquid air temperature are given in fig. 6.

At the lowest target temperature used the results were not reproducible, although there seems to be a tendency toward higher values of S when a (110) copper crystal is used and lower values of S when a (111) copper crystal is used. The boiling point of Ar is 9° above the boiling point of normal air. It may be possible that argon gives rise to contamination of the surface by two dimensional condensation. This in spite of the high efficiency for surface cleaning by the Ar^+ ion beam. When the Ar content in the first target atom layers is not liberated by diffusion, as it is at higher temperatures, we can imagine a decline of the crystal order which will tend to diminish the difference in sputtering ratio for differently orientated single crystals.

Because of these considerations further experiments were performed with Ne, which has a boiling point which is more than 50° below the boiling point of normal air.

Sputtering ratios from 20 keV Ne^+ ions for temperatures down to the lowest value which could be reached with liquid hydrogen without decreasing the ion beam intensity too much are given in fig. 7. We conclude from these measurements that there are three different temperature ranges, in which the sputtering ratio changes in a given way, independent of the orientation of the lattice atoms of the copper*), namely

1. a decrease of S from 150° to 100°K.
2. an increase of S from 100° to 60°K.
3. a decrease of S from 60° to 20°K.

The second temperature range, where the sputtering ratios increase for lower target temperatures, can be a range in which the surface density is increased by an increase of the noble gas content. This

---

*) A decrease of S is found from 320° to about 250°K which appears only for the (111) crystal. Although, it may be possible that it can be understood by a mechanism which involves the migration of vacancies, it will not be considered anymore. Its magnitude is only slightly above the accuracy of the measurements.
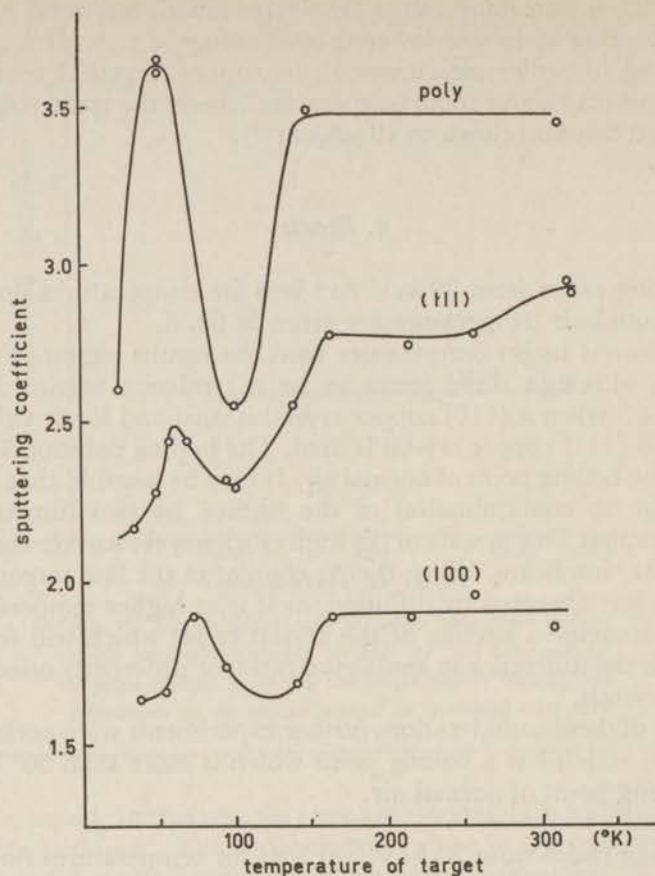
Fig. 7. *The sputtering ratio of copper targets for different target temperatures during 20 keV Ne⁺ ion bombardment. The three curves correspond to measurements on a polycrystalline target, a single crystal with a (111) surface and a single crystal with a (100) surface.*

will cause a decrease of the penetration depth and consequently an increase in sputtering yield. To verify this assumption the following experiment was performed.

Copper disks were thoroughly outgassed in a vacuum oven for several days. Afterwards the outgassed pyrex vessel, shown at the right side of fig. 8, was used for further outgassing by high - frequency heating. Many times the copper disk was heated to red heat (> 600°C), which was maintained for several hours. In this way it was possible to get a polycrystalline copper target with relatively large crystallites, from which no detectible quantity of gas could be liberated at a temperature of about 600°C. This temperature of

42

600°C is reached in 10 s by high-frequency heating, as denoted at the time axis of fig. 9.

This degassed target is bombarded with 20 keV Ne+ ions for several hours during which the Ne content of the target has reached almost its saturation value. Compare e.g. the collection curve, measured by Almén and Bruce[1]), for Ne in Ta by 45 keV Ne+ ion bombardment, which shows that saturation is reached in two hours when the current density was a factor of ten lower than that used in our investigation. The saturation value for 20 keV Ne+ on copper can be estimated to be 0.7 $\mu g/cm^2$ by linear interpolation between the value for 45 keV Ne+ as measured by Almén and Bruce and 0 keV. This interpolation seems to be justified by the linear dependence of the saturation value for Kr+ ions on Ag between 20 and 50 keV[1]). Because of this we expected in the pyrex vessel of 105 cm^3 volume a maximum Ne pressure of 12×10^{-3} torr.

We remark here that Almén and Bruce also measured a decrease of the saturation value of Kr for 45 keV Kr+ ions on Ag and Cu of the order of 30% when the target temperature was raised from 300° to 700°K.

To prevent contamination of the outgassed inner wall of the pyrex vessel the copper target is brought into the vessel under high vacuum. This could be performed by putting the target in position I (cf. fig. 8) followed by pumping of compartment A after which the one

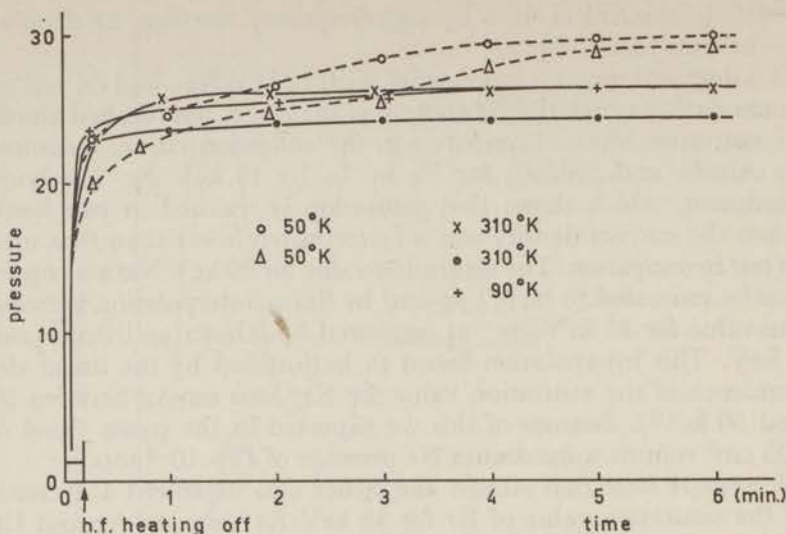Fig. 8. Apparatus for the determination of the noble gas content in ion bombarded copper targets.
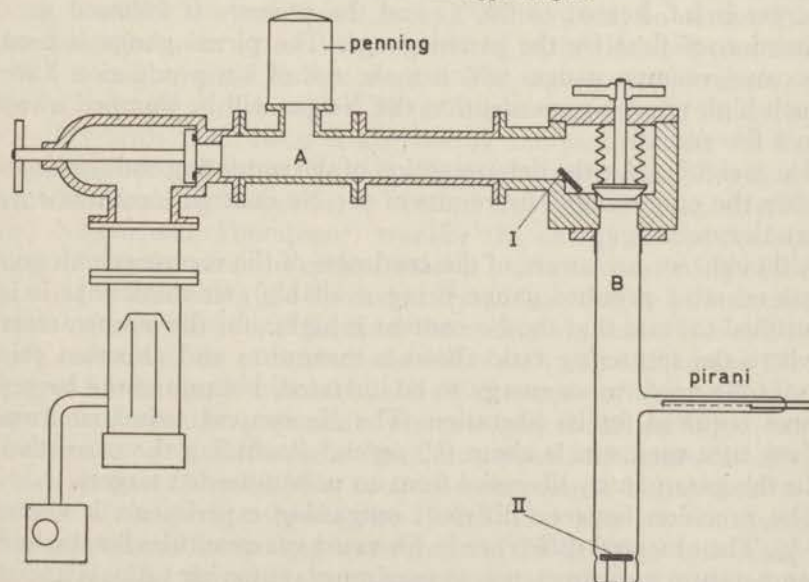
Fig. 9. The pressure of the gas liberated from Ne bombarded copper targets, by 10 second high-frequency heating, as a function of the time which passed after the heating was started. Different curves belong to different temperatures at which the target was bombarded with the 20 keV Ne+ ions.

inch bakeable Edwards valve between compartment A and B is opened. The valve is closed when the target is in position II. The target is h.f. heated to 600°C and the pressure is followed as a function of time by the pirani gauge. The pirani gauge is used because vacuum gauges which make use of ion production have such high pumping speeds, that the Ne gas will be pumped away in a few seconds.

The weighing, for the determination of the sputtering ratio, is done after the outgassing. The results of the Ne content measurements are shown in fig. 9.

Although, we are aware of the crudeness of the measurements (no gas selective pressure gauge being available), we think that it is justified to state that the Ne content is higher for the temperatures where the sputtering ratio shows a maximum and also that this extra Ne needs more energy to be liberated, because of the longer time required for its liberation. The Ne content estimated from these measurements is about 0.9 μg/cm^2 (including the correction for the gas quantity liberated from an unbombarded target).

The precision between different outgassing experiments is about 5%. The observed difference in liberated gas quantities for the low temperature measurements, at maximum sputtering ratio, is about

44

10%. The gas liberated from an unbombarded target which was treated in the same way as a bombarded one, except for its situation in the separator, is 30% of that obtained from a bombarded target. This 30% value is not appreciably different for various experiments. Measurements were also done with 20 keV He+ ions. The target contained, as a maximum, an 8 times higher gas concentration. Unbombarded targets contained only about 6% of the amount of gas measured with a bombarded one, but the precision was not improved. It was not possible to detect a difference in noble gas content for different target temperatures during bombardment. It is assumed that the condition of the copper surface during the bombardment with He+ ions is the reason for this negative result. The sputtering efficiency of He for surface cleaning is very low and the copper surface was mostly blue after the bombardment, probably due to the formation of oxide layers. Consequently the determination of a reliable sputtering ratio was also impossible. We remark here that, if this contamination could be avoided, one could expect to find the same dependence of the sputtering ratio as a function of target temperature for He and Ne, because both will be in interstitial positions in the copper lattice when no vacancies are in the neighbourhood[9]).

5. Discussion

A decrease in S at decreasing temperature is possibly caused by the influence of displacements of the lattice atoms. Suppose Frenkel pairs, made by the recoil particles of a primary ion, do not annihilate by diffusion in a time short compared to the time between two ion hits in the same surface region. The mean concentration of interstitials will then increase. These interstitials and the vacancies together with their stress fields destroy the lattice order in the neighbourhood of the surface, i.e. the region important for sputtering. The focusing collisions, as treated by Silsbee[10]), Leibfried[11]) and Nelson and Thompson[5]) transfer the energy to the surface most efficiently when the crystal order is perfect. A scattering of the focusing chains along the low index crystal axes due to an accumulation of interstitials will decrease the sputtering ratio. The steady state concentration of interstitials will clearly depend on the lifetime of Frenkel pairs created by the recoil atoms and the bombarding flux. From the arguments presented by Leibfried[12]) we can visualize a region in the metal (area for normal incidence 5000 Å²), which contains Frenkel pairs to a concentration of 1% as a consequence of the penetration of one 10 keV Cu+ ion. We will make this supposition to analyse our results of 20 keV ion sputtering, since it can be shown that the magnitude of this area, normal to

the ion direction, is relatively insensitive to energy changes from 10 to 40 keV.

We will now follow the analysis of interstitial diffusion as a function of metal temperature as given by Sanders[13]). In the diffusion equation $\delta n / \delta t = D \, \Delta n$ (n = density of interstitials) the coefficient of diffusion is

$$D = D_o \exp\left(-\varepsilon/kT\right) \tag{1}$$

where ε is the activation energy for the diffusion of interstitials. Using diffusion values from Wert and Zener[14,15]) we find

$$D_o = 0.44 \times 10^{14} \sqrt{\varepsilon} \cdot e^{3\varepsilon} \; (\text{Å}^2/\text{s}) \tag{2}$$

for diffusion of copper interstitials from b.c. positions in a copper lattice. By b.c. position is meant the body-centered position in the center of a unit cell. Sanders[13]) solved the diffusion equation for the 5000 Å^2 region mentioned above and found for the time dependent factor of the concentration

$$e^{-D\mu^2 t}, \text{ when } \mu^2 = 0.02 \; \text{Å}^{-2}. \tag{3}$$

For a beam current in the order of 100 μA/cm^2 the mean time difference between the arrival of two successive ions in the area of 5000 Å^2 is $t_o = {}^1/_{320}$ s. Substitution of t_o for time t in (3) gives the relative concentration f remaining after this time:

$$f = \exp\left(-D \cdot 6.56 \times 10^{-5}\right).$$

For prolonged ion bombardment we then obtain

$$\frac{n_{t_o}}{n_o} = \frac{1}{1-f} = \left[1 - \exp\left(-D \cdot 6.56 \times 10^{-5}\right)\right]^{-1} \tag{4}$$

in which n_o is the concentration of interstitials caused by one bombarding ion directly after its penetration into the metal. Substitution of (1) and (2) in (4) gives

$$\frac{n_{t_o}}{n_o} = \left[1 - \exp\left\{-2.91 \times 10^9 \sqrt{\varepsilon} \exp\left(-\frac{11\,605}{T}\,\varepsilon + 3\varepsilon\right)\right\}\right]^{-1} \tag{5}$$

where ε is in eV and T in degrees Kelvin.

The inverse of the right hand side of equation (5) i.e. $(1 - f)$ represents the mean fraction of interstitials which have been annihilated by vacancies during the time t_o. We propose that the ratio n_{t_o}/n_o must change drastically before it will have an effect on sputtering, because an increase of $\approx 10\%$ of n_{t_o} only changes the supposed concentration of Frenkel pairs[12]) from 1% to 1.1%, which should not cause a measurable change in the sputtering ratio.

Taking the maximum change in $(1 - f)$ at the temperature T_o, below which the influence of interstitial accumulation will be
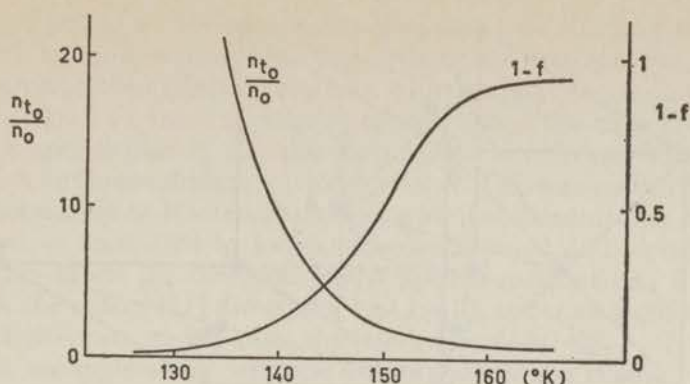
Fig. 10. *The steep increase of the relative concentration of interstitials n_{t_0}/n_0 in copper, when the target temperature is below $150°K$ during bombardment. n_0 is the maximum concentration of interstitials caused by the penetration of a single ion. n_{t_0} is the equilibrium concentration of interstitials caused by projectiles arriving in the same area at average time intervals t_0.*

---

measurable in S, we get, by repeated differentiating for T of the inverse of the right hand side of equation (5) and equalizing to zero, the equation

$$1 - \frac{2T_0}{11\ 605\ \varepsilon} = 2.91 \times 10^9 \ \sqrt{\varepsilon} \ \exp\left[\left(-\frac{11\ 605}{T_0} + 3\right)\varepsilon\right] \quad (6)$$

or approximately

$$\frac{11\ 605\ \varepsilon}{T_0} = 21.9 + \tfrac{1}{2} \log \varepsilon + 3\varepsilon. \quad (7)$$

Here T_0 will represent the temperature at which the steepest change of $(1 - f)$ *vs* T will occur. On the basis of the measurements shown in fig. 7 we chose the experimental value of $150°K$ for T_0, since this represents the point at which a qualitative change in the behaviour of S *vs* T is observed. This value of T_0 substituted into (7) gives an activation energy $\varepsilon = 0.29$ eV and leads to the concentration behaviour shown in fig. 10.

Possible errors introduced during the calculation are: the error in the temperature measurement, deviations in the beam current from $100\ \mu A/cm^2$, the calculation of the area containing interstitials, the choice of the distance of possible neighbouring interstitial positions, and the choice of T_0 from the measured curve $S\ (T)$.

The relative unimportance of an error in the area containing interstitials and in the beam current can be shown by varying, in eq. (5), the T together with the area and beam current, which are contained in the factor 2.91×10^9. A factor of 6 in the area, in the
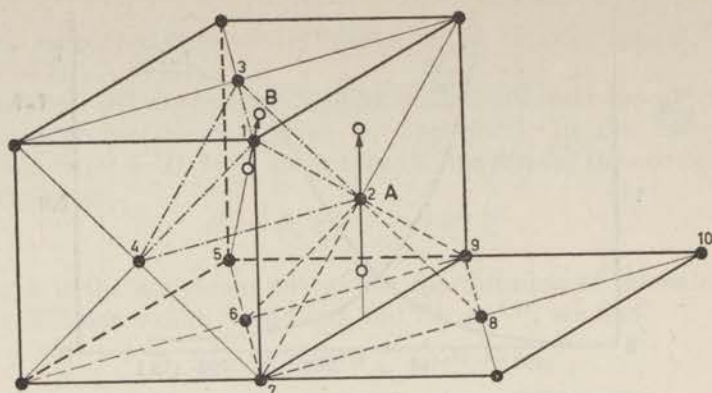
47

Fig. 11. A representation of a unit cell of copper with possible interstitial configurations of copper atoms. The black dots represent the normal lattice sites. The A interstitial configuration, represented by the hollow circles above and below the equilibrium position 2, can be created by bringing an interstitial atom from below to the position of the lower hollow circle. This will in turn displace the atom originally located at 2 to the position indicated by the upper circle. It can be shown that the lower circle lies almost at the center of gravity of the pyramid 2—6—7—8—9. Similarly, the B interstitial configuration is created by the displacement of atom 1 by the interstitial atom indicated by the hollow circle below position 1. The equilibrium position for this lower circle lies approximately at the center of the tetrahedron 1—2—3—4[17,18]).

beam current, or in the distance of neighbouring interstitial positions corresponds to a change of 5° in T. It seems reasonable that the total error in T_0 including all these errors is $\pm 10°$ in T_0. This corresponds to an error in ε of only 0.02 eV. i.e.

$$\varepsilon = (0.29 \pm 0.02) \text{ eV.}$$

Results from radiation damage experiments[16]) about thermal recovery of damage caused by 12 MeV deuterons in copper at 123° and 133° K can probably be related to the process discussed above. The recovery measurements were described with an activation energy $\varepsilon = (0.20 \pm 0.05)$ eV.
Calculations of Bennemann[17,18])showed the stability of an interstitial split configuration at the corner of a copper unit cell along a [111] direction. The activation energy for the diffusion of this so-called B interstitial was estimated at 0.30 eV.
For the (111) copper surface the relative decrease of S below 150°K was about twice that of a (100) copper surface (cf. fig. 7). We can

48

ascribe this to a difference in the probability for forming B interstitials by the following reasoning. Distant encounters of the nearly unperturbed fast injected ions with lattice atoms give recoil copper particles with a small amount of energy into a direction more or less perpendicular to the direction of the ion beam. The cross-section for these collisions is relatively large. This mechanism favours the formation of B interstitials during ion bombardment of a (111) crystal as compared to ion bombardment on a (100) crystal. Cf. fig. 11: When the direction of the normal incident ions is along 1—5, the other [111] directions, e.g. 1—10, are at an angle of 71°, which is closer to 90° than the [100] directions, e.g. 1—7, which make an angle of 55° with the direction of the ion beam.

For normal incidence on a (100) crystal, say direction 1—7, the [111] direction along 1—5 is at 55° and the [100] direction is normal to the direction of the incoming ion, thus tending to favour the formation of A interstitials.

Another contribution to the difference in the magnitude of the decrease of S below 150°K for different crystal orientations is the change of opacity by a fixed amount of interstitials. If the total concentration of interstitials (A and B species taken together, cf. fig. 11) is independent of crystal orientation, the decrease of penetration depth of the incoming ion is more important for an open direction. This influence will tend to increase the sputtering ratio. This, balanced against the influence of interstitials on focusing chains, will also result in a smaller decrease below 150°K for the (100) crystal.

The increase of S below 100°K has been ascribed to an increase in the surface density by an increasing amount of Ne gas. The penetration depth of the incoming ion decreases and sputtering increases independent of the actual orientation of the copper. This increase of the Ne content of the target was verified for polycrystalline copper (cf. fig. 9).

According to theoretical calculations of Rimmer and Cottrell[9]), on the solubility of noble gases in copper, the estimated energy for substitutional solution is 5.9 eV and for interstitial solution 4.6 eV. This means that Ne will diffuse as an interstitial, probably with a low activation energy compared to copper interstitial activation energies. Accumulation of Ne interstitials in the temperature range where the experiments were performed is not expected. However, because of the accumulation of B interstitials which are substancially immobile below 120°K, the concentration of vacancies has been increased. When a vacancy is present the energy for substitutional solution is 1.5 eV[9]) and the Ne will be trapped by these vacancies. This can account for an extra amount of Ne in the target, which is liberated more slowly by heating than the interstitial Ne in accordance with the measurements shown in Fig. 9. This would only

be true if the density of vacancies increases much more slowly with decreasing temperature than the interstitial concentration.

The so-called A interstitial of copper (cf. Fig. 11) in a copper lattice, a split configuration along a [100] direction with an activation energy of 0.1 eV, is also calculated as a stable configuration[19, 17,18]. The A interstitials, having a low activation energy, are only important in the lowest temperature region at about 50°K. The freezing of these interstitials introduces further disorder. The decrease of the sputtering ratio for lower target temperatures in this temperature region may be related to this extra disorder. The existance of a high concentration of A interstitials was also confirmed by low temperature radiation damage experiments, in which sharp electrical resistance changes were observed following annealing at 40°K[20].

The relative probability for the formation of A interstitials as a function of the direction of the injected ion beam can be understood by the same reasoning that was applied for the B interstitials.

Finally, we want to point out that A and B interstitials seem to be equally important for sputtering of copper, whereas A interstitials are relatively much more dominant in annealing of radiation damage.

REFERENCES

1. Almén, O. and Bruce, C., Nucl. Instr. and Methods **11** (1961) 257
2. Rol, P. K., Private communication.
3. Nelson, R. S., Thompson, M. W. and Montgomery, H., Phil. Mag. **7** (1962) 1385.
4. Sanders, J. B. and Fluit, J. M., to be published in Physica.
5. Nelson, R. S. and Thompson, M. W., Proc. Royal Soc. A, **259** (1961) 458.
6. Fluit, J. M. and Rol, P. K., to be published in Physica.
7. Handbook of Chemistry and Physics, Thirty-Ninth ed., Chemical Rubber Publ. Co., Cleveland, Ohio, p. 2419.
8. Rol, P. K., Fluit, J. M. and Kistemaker, J., Physica **26** (1960) 1000.
9. Rimmer, D. E. and Cottrell, A. H., Phil. Mag. **2** (1957) 1345.
10. Silsbee, R. H., J. Appl. Phys. **28** (1957) 1246.
11. Leibfried, G., J. Appl. Phys. **30** (1959) 1388.
12. Leibfried, G., Lectures on Radiation Damage, Summer School at Ispra, 1961.
13. Sanders, J. B., Le Bombardement ionique, colloque international, Bellevue 1962. Ed. Centre National de la Recherche Scientifique, Paris 1962, p. 125.
14. Wert, C. and Zener, C., Phys. Rev. **76** (1949) 1169.
15. Zener, C., Imperfection in Nearly Perfect Crystals, Wiley, New York.
16. Marx, J. M., Cooper, H. G. and Henderson, J. W., Phys. Rev. **88** (1952) 106.
17. Bennemann, K. H., Phys. Rev. **124** (1961) 669.
18. Bennemann, K. H., Z. f. Physik **165** (1961) 445.
19. Gibson, J. B., Goland, A. N., Milgram, M. and Vineyard, G. H., Phys. Rev. **120** (1960) 1229.
20. Billington, D. S. and Crawford Jr., J. H., Radiation Damage in Solids, Princeton University Press, Princeton, 1961, p. 118.

THE EMISSION OF FAST SECONDARY ATOMS FROM IONICALLY BOMBARDED COPPER ("REFLECTIONS")

1. *Introduction*

A lack of knowledge about the emission of fast secondary atoms during sputtering experiments can give rise to misunderstanding of the results of these sputtering experiments. E.g. measurements of the mean velocity of sputtered particles can be highly in error when they are done at angles favourable for the ejection of "reflected" atoms[1,2]. Measurements of the angular distribution of sputtered particles by collection of these particles on plates, can be influenced substantially by the sputtering action of the "reflected" particles. Furthermore "reflected" atoms influence the energy balance to about the same extent as the sputtered particles. Also the surface roughness of a sputtering target will be changed when "reflected" particles cause secondary sputtering, which may have a measurable influence on the sputtering ratio and on the angular distribution of sputtered particles.

A fundamental approach to the investigation of the penetration of fast particles in solid material is also possible by the study of "reflected" particles from surface atom layers. The results described in this chapter will have to be extended with more accurate experiments in which ionizing of the emitted atoms permits an accurate energy and mass selection. This energy selection was not possible in the experiments described here, as secondary emission of electrons was used for the detection of the reflected particles. The secondary emission coefficient could not be determined in the magnetic field of the isotope separator in which the experiments were performed.

2. *Apparatus and operational measurements*

The apparatus consisted of a sputtering target which could be rotated in the vacuum system of the electromagnetic isotope sepa-
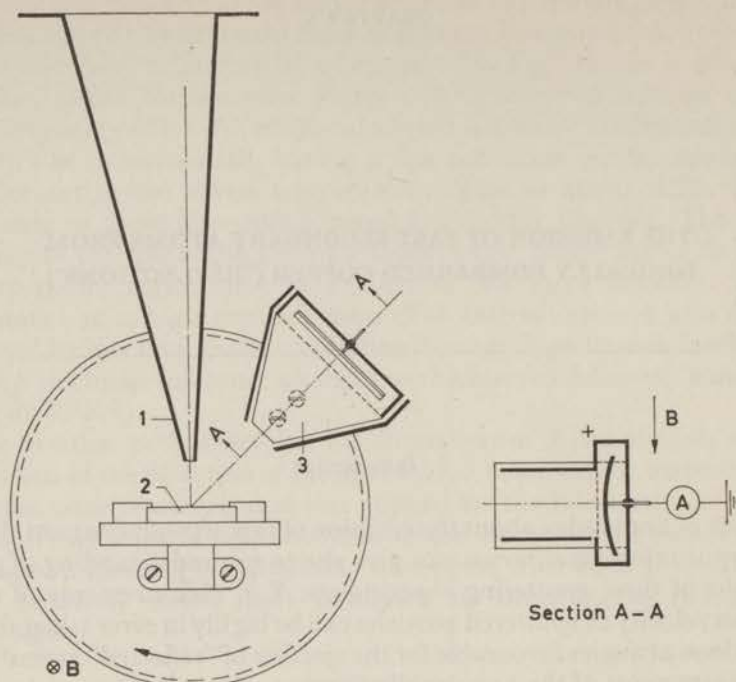
Fig. 1. Schematic of the experimental set up: The diaphragm
(1) is at a fixed position. The target (2) is mounted on a wheel
or just above it, with its centre in the middle of the target
surface where the ion beam hits. The detector house (3) is
mounted on the wheel. The section A-A of the detector shows
the curved detector plate from which secondary electrons are
drawn to the positively charged house. Deflection plates and
screening plates are shown.

rator, permitting a simple and rapid change of the angle of incidence
of the primary ion beam on the target (fig. 1). The fast secondary
particles were measured by a detector consisting of a shielded
convex copper plate. The angular dependence of the "reflected"
particles was measured with target and detector fixed on a wheel,
so that the measurements were always done at a detection angle of
45° with the target surface in a plane perpendicular to the rotation
axis of the target. The scattering angle was 135°-φ where φ, the
angle of incidence of the primary ions, is defined with respect to
the normal on the target surface. When the angular distribution of
the "reflected" particles is measured the target is loosened from the
wheel and put in a fixed position with respect to the ion beam.
The target and detector mount as shown in fig. 1 were mostly
situated in a magnetic field of approximately 1000 gauss. The

convex detector plate permits, in the magnetic field, the escape of secondary electrons produced by collisions of fast atoms or ions with the copper surface of the detector. The secondary emission coefficient was estimated to be in the order of 1[3]), which means that the amount of secondary electrons can be identified more or less, with the amount of "reflected" particles.

A concave detector plate was used to determine the current of electrons, or positive, or negative ions coming into the detector system. A small negative current was observed which could be minimized by the use of deflection plates supplying an electric field parallel to the magnetic field.

Screening plates perpendicular to the former ones proved their importance against double reflections. (Cf. fig. 4: the signal at $\Theta = 90°$ was much larger when no screening plates were used.)

To determine the velocity of the detected fast particles a pulsed beam technique was used. Deflection plates were built in the middle of the 180° isotope separator, where the space charge of the ion beam is a minimum because of the large beam spread. Electrical pulses applied to the plates were able to deflect the beam in a time somewhat shorter than one μs, if the ion-source operates under favourable conditions (little hash). This was used to measure the time delay between the target- and the detector signal. The build up of the space-charge compensated ion beam takes some hundreds of μseconds and is not suitable for the time delay measurement. The measured time delay for a 15 keV Ar$^+$ ion beam on Cu at 7 cm target-detector distance was about 0.3 μs, from which follows a high particle velocity comparable with the initial ion velocity.

To improve the accuracy of the velocity measurement the whole system was enlarged to realize a target-detector distance of 70 cm. The time difference between target pulse and detector pulse can be determined with an accuracy of 0.1 μs. The enlargement of the distance with a factor 10 makes it thus possible to measure the time of flight with an accuracy of about 5%, corresponding to an energy determination of the fast particles with an accuracy of 10%. The measured time delays for 10, 14.2 and 19.9 keV primary Ar$^+$ ions on Cu are respectively 3.4, 2.8 and 2.3 μs, corresponding to secondary Ar particles with 8.8 keV, 13.0 keV and 19.1 keV energy. We conclude from these measurements that the detected fast particles are Ar particles. Cu particles with the measured velocities have an energy which is about 20% above the initial Ar$^+$ ion energy.

The primary ion beam was deflected by the solid target into the detector over an angle of 40° for the enlarged experimental arrangement. An Ar particle scattered by a single elastic collision with a Cu atom of the solid looses $\frac{1}{4}$ of its energy when it is scattered over 40°. This means that we may expect that a large part of the "reflected" particles are arising from those Ar$^+$ ions which made a
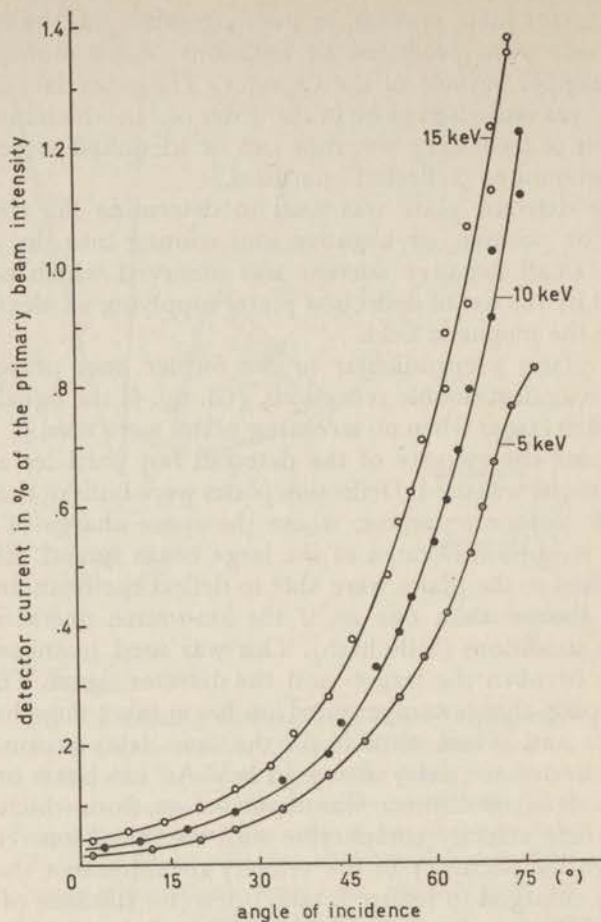
Fig. 2. Production of fast secondary particles as a function of
the angle of incidence φ of an Ar⁺ ion beam on a polycrystalline
Cu target. Solid angle of detection 0.02 steradian.

single elastic collision at the surface layers of the Cu target.
In case of the large distance between target and detector the Ar
particles travel through the stray field of the isotope separator and
the ions cannot reach the target. This could be proved by using
large electrical deflection plates. The amount of ions was measured
roughly on bended plates at the side of the path of the secondary
Ar atom beam. We measured an amount of 10—15% secondary Ar⁺
ions relative to the secondary atoms, both of about the same energy.

54

3. *Angular dependence measurements and discussion*

The angular dependence of the secondary Ar (Ar+) particles of high velocity was measured with polycrystalline and with single crystalline copper targets. These measurements were performed always with a target-detector distance of 7 cm.

Results for 5, 10 and 15 keV primary Ar+ ion energy are given in figs. 2 and 3. The width of the detector slit corresponds with an angular interval $\Delta \Theta$ of 4°, if Θ is the angle between the direction target-detector and the normal on the target.

The angular distribution of fast secondary particles was measured for different angles of incidence of the primary Ar+ ion beam. The results are shown in fig. 4.

The sharp rise of the yield of fast particles with increasing incidence angle of the ion beam (fig. 2) is in relative numbers about a factor of ten higher (at $\Theta = 45°$) than the corresponding rise of the total yield of sputtered particles[4]).

Fig. 3. Production of fast secondary particles as a function of the angle of incidence φ of an Ar+ ion beam on a (100) Cu surface, turned about a [001] direction. Solid angle of detection 0.02 steradian. $\Delta \Theta = 4°$.
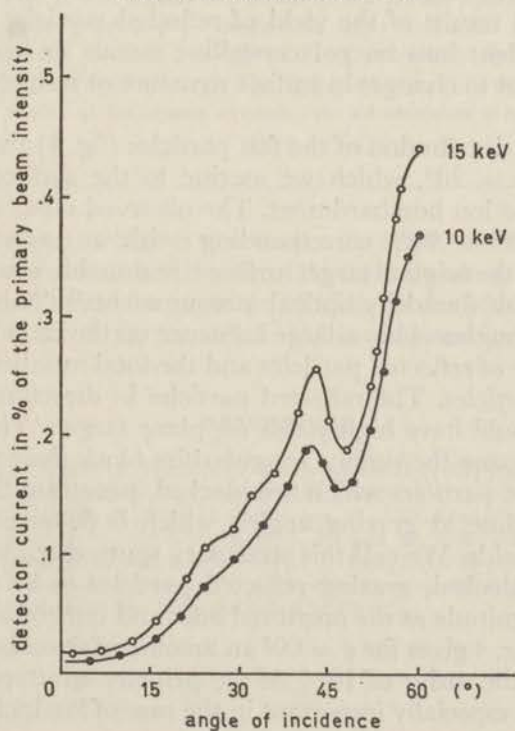
A number of bi-particle collisions between Ar and Cu give rise to a forward peaked fast particle distribution. In the case of sputtering however, this particle distribution will be almost spherical as the process takes place deeper inside the crystal.

The minimum in the yield of fast particles found for primary ion incidence along the open crystal direction [110] (fig. 3, $\varphi = 45°$) corresponds to a deeper penetration of the primary ion in the crystal, just as was found for the yield of sputtered particles as a function of the angle of ion incidence[5]. The minimum is much less pronounced than the one measured for the sputtering yield. This is in accord with the assumption that only single and double collisions from the first two or three lattice layers contribute to the emission of fast particles. From the relative depth of the minimum we deduce that about 25% of the total number of "reflections" arises from collisions with deeper layers (which are screened by the first layer when ions penetrate along the [110] direction). We see from fig. 3 that the chance of reflection from deeper layers diminishesquickly with the energy. (Cf. the relative depth of the curves in fig. 3). Because of the existence of this minimum and because of the small energy spread in the reflected ions, which follows from the time delay measurements, we cannot expect more than 10% double collisions.

Mashkova *et al*[6]) ascribes the difference between theoretical and experimental results of the yield of reflected particles for 30 keV grazing incident ions on polycrystalline metals to secondary collisions and not to changes in surface structure or influence of lattice order.

The angular distribution of the fast particles (fig. 4) shows a maximum for $\Theta = 70°$, which we ascribe to the surface roughness caused by the ion bombardment. The observed effect of 20° blind direction $(70° \rightarrow 90°)$ corresponding with an average surface roughness of the original target surface is reasonable when compared with the result found by optical measurements[7]. This means that the surface roughness has a large influence on the ratio between the total number of reflected particles and the total number of the slow sputtered particles. The reflected particles in directions for which $\Theta > 70°$ should have high yields for plane targets. These are not observed because the surface irragularities block their path.

However, the particles which are blocked, penetrate the metal for the second time at grazing angles, which is favourable for high sputtering yields. We call this secondary sputtering. Assuming the number of blocked, grazing reflected particles to be of the same order of magnitude as the measured ones and integrating the yields as given in fig. 4 gives for $\varphi = 60°$ an amount of secondary sputtered particles in the order of 10% of the primary sputtered particles. This effect is especially important in the case of ion incidence along
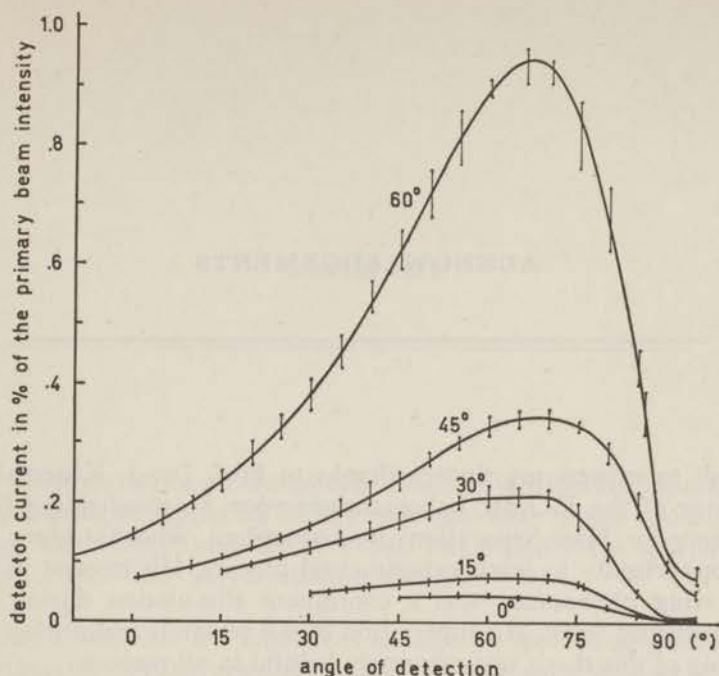
Fig. 4. The angular distribution of fast secondary particles emitted from a polycrystalline Cu target bombarded with 15 keV Ar⁺ ions. The different curves correspond to different angles of ion incidence φ. The angle of emission, Θ, is defined positive in the opposite direction from the normal as is taken for φ.

a [110] direction, where S decreases a factor 4, but the intensity of reflected particles only a factor 1.5 corresponding to a possible contribution of secondary sputtering of the order of 30%. This may be related to the flatter surface found in that case[7]).

REFERENCES

1. Almén, O and Bruce, G., Nucl. Instr. and Methods **11** (1961) 257.
2. Kopitzki, K. and Stier, H. E., Z. Naturf. **17a** (1962) 346.
3. Cousinié, P., Combié, N., Fert, C. and Simon, R., C.R.Acad. Sci. **249** (1959) 387.
4. Rol, P. K., Fluit, J. M. and Kistemaker, J., Physica **26** (1960) 1000.
5. Fluit, J. M., Rol, P. K. and Kistemaker, J., J. Appl. Phys. **34** (1963) 690.
6. Mashkova, E. S. and Molchanov, V. A., Soviet Physics-Doklady **7** (1963) 829.
7. Fluit, J. M. and Datz, Sh., to be published in Physica.

57

ACKNOWLEDGEMENTS

58

SUMMARY

This thesis describes measurements concerning different aspects of the sputtering of copper by 20 keV noble gas ions. Single crystalline copper was mostly used, for it reveals much better the sputtering characteristics than polycrystalline material.

Chapter I describes the important changes in sputtering yield of a single crystal for different directions of ion incidence. Copper single crystals were bombarded with 20 keV Ne^+, Ar^+ and Kr^+ in a 180° isotope separator. Measurements of sputtering yields were made at different angles of incidence of the noble gas ions impinging on the surface of a copper single crystal. We made use of three differently oriented crystals with a (100), (110) and (111) plane as a surface. The yield-angle curves show relative minima at incidence angles where the ion beam is aimed along low index crystal directions. The width of the minima and the angle at which a minimum occurs is discussed in terms of a rigid sphere model of the surface region, where the chance of a collision in this region is taken as the most important parameter for the sputtering ratio. This model enables us to derive an effective collision radius from the experimental data. This method yields, for 20 keV Ne^+, Ar^+ and Kr^+ ion bombardment on Cu, effective collision radii of 0.25 Å, 0.29 Å respectively 0.24 Å, which is a factor 2.1, 1.7 respectively 1.0 higher than that obtained from the Bohr theory in the hard sphere approximation. A physical interpretation of these factors indicates that the used model is not entirely applicable.

Chapter II describes the micro relief of ionically bombarded copper for different crystal orientations with respect to the ion beam direction. Optical examination of the surface of a (100) Cu single crystal which had been bombarded by 20 keV Ar^+ ions revealed structure which was dependent on the incidence angle of the ion

59

beam. For incidence angles corresponding to small ion penetration depth the structure could be explained on the basis of two competing mechanisms; one favouring the development of facets normal to the ion beam and the other favouring the development of (110) facets. Qualitatively different behaviour was found when the ion beam was directed at 45° to the surface (corresponding to a [110] crystal direction). This difference has been attributed to the large increase in mean penetration depth for this incidence angle.

Chapter III treats a direct ejection mechanism of slow surface atoms. Sputtering by small momentum transfers to surface atoms is a well known mechanism in low energy, but not in high energy sputtering. At higher primary ion energies particles are ejected from inside the crystal and for oblique ion incidence no preferential ejection direction is known for polycrystalline metals. In this chapter we discuss a special arrangement to detect preferential ejection directions due to small momentum transfers to surface atoms, caused by 20 keV Ar+ ion bombardment on monocrystalline copper. Preferential ejection was found normal to the direction of the ion beam. The integrated contribution of this sputtering mechanism to the total sputtering ratio is estimated to be 0.7, which is in accordance with theoretical expectations based on the large cross-sections valid for these small energy transfers.

Chapter IV describes the influence on the sputtering yield of the temperature of the copper target (40°—900°K). Sanders calculated the range of focusing collision sequences in [110] directions for copper, taking into account thermal vibrations. An average range of 5 atomic distances was found for room temperature. This small number, which decreases for higher metal temperatures, can be correlated to an almost temperature independent sputtering ratio between 300° and 900°K. This fits with the experimental results of sputtering ratio measurements for target temperatures between 300° and 600°K.
Single crystals of copper and polycrystalline copper were bombarded at normal incidence with 20 keV Ar+ and Ne+ ions at various temperatures between 30° and 320°K.
The sputtering ratio, S, for Ar+ ions on polycrystalline targets as well as on monocrystalline surfaces showed no temperature dependence within the accuracy of measurements between 80° and 350°K.
Bombardment with Ne+ ions in the temperature range between 30° and 350°K on polycrystalline Cu and on (111) and (100) single crystal surfaces showed a very pronounced temperature dependence below 200°K.
An explanation is given on the basis of internal focusing mechanisms inside the crystal. A steep decrease in S observed below 150°K is

related to the diffusion of the so-called B interstitials in the Cu lattice. On this assumption, the measurements yield an activation energy of (0.29 ± 0.02) eV for the diffusion process. A second steep decrease of the sputtering coefficient below $50°K$ can be due to the decreased diffusion of A interstitial copper atoms (activation energy 0.1 eV). A sharp rise in S going from about $100°K$ to $50°K$ probably corresponds to an increasing saturation of the copper lattice with Ne. This was verified by measurement of the gas content present in the targets following bombardment.

Chapter V describes a study of the production of fast secondary atoms from copper polycrystalline and single crystalline targets. The "reflected" atoms were measured with a secondary emission detector. The targets were bombarded with Ar^+ ions, mainly at an energy of 15 keV.
We found, by application of pulsed ion beam techniques that the energy distribution of the measured atoms has a sharp maximum at the mean value expected for single elastic bi-particle collisions. The total yield of these "reflections" was measured as a function of the angle of incidence of the ion beam. It increases much faster than the sputtering ratio and reaches a value of more than 1% of the primary ion beam for very oblique incidence. Experiments on a single crystal show the influence of crystal orientation on the "reflections". The influence of crystal order is much smaller than the analogous one for sputtering. This shows that the process of sputtering of neutral copper atoms takes place deeper inside the crystal than the emission of fast particles. Most "reflected" atoms were found at a "reflection angle" of $70°$ with the normal, independent of the angle of incidence of the primary ion. The maximum "reflection" angle will be determined by the surface roughness, which is not strongly dependent on the angle of incidence for polycrystalline targets. An estimate of secondary sputtering due to the "reflections" and the surface roughness gives a yield in the order of 10% of that from primary sputtering.

SAMENVATTING

Dit proefschrift beschrijft verschillende aspecten van de verstuiving van monokristallijn koper door edelgasionen.

In hoofdstuk I wordt nagegaan welke verandering van de verstuivingsopbrengst optreedt als de ionenbundel verschillend georiënteerd is ten opzichte van een koper-monokristal. Metingen werden uitgevoerd met 20 keV Ne+, Ar+ en Kr+ bundels in een 180° isotopenseparator. Verstuivingsverhoudingen werden gemeten voor verschillende invalshoeken van de ionen op (100), (110) en (111) vlakken van koper. Relatief zeer lage verstuivingsverhoudingen werden gevonden voor die invalsrichtingen, die samenvallen met laag geindiceerde kristalrichtingen. Ook in een vrij breed hoekgebied om de genoemde richtingen is de verstuivingsverhouding laag. Dit wordt toegeschreven aan de verminderde botsingskans in de eerste atoomlagen van het kristal voor ionen, die langs deze richtingen binnentreden. Het hoekgebied, waarin relatief lage verstuiving optreedt, hangt dan samen met de richtingen, waarin naburige atomen geheel of gedeeltelijk achter elkaar liggen. Het is dan mogelijk een effectieve botsingsdoorsnede te bepalen. Uit de meetresultaten volgt volgens deze methode een effectieve botsingsstraal van 0,25 Å, 0,29 Å en 0,24 Å respectievelijk voor 20 keV Ne+, Ar+ en Kr+ ionenbeschieting op koper. De Bohr-theorie geeft voor deze energie harde bol stralen van respectievelijk 0,12 Å, 0,17 Å en 0,23 Å. Een interpretatie van de onderlinge verschillen wordt gegeven op basis van de ontoereikendheid van het gebruikte model.

In hoofdstuk II wordt nader ingegaan op het reliëf van het oppervlak van een monokristal, zoals dat ontstaat na ionenbeschieting. Optisch onderzoek van het oppervlak van een (100) koperkristal, dat in verschillende richtingen beschoten werd met 20 keV Ar+ ionen toonde systematische verschillen. De sterkste onregelmatig-

62

heden werden gevonden voor die richtingen, waarbij het ion grote botsingskansen in de eerste atoomlagen van het kristal heeft. De richting, waarin de vlakjes dan staan, kan verklaard worden uit een voorkeur voor het ontwikkelen van vlakken loodrecht op de bundel gepaard gaande met een voorkeur voor het ontwikkelen van (110) vlakken.

Hoofdstuk III behandelt verstuiving veroorzaakt door kleine energie-afgiften aan oppervlakte atomen door de hoogenergetische ionen (20 keV). Deze verstuiving is niet eerder opgemerkt, omdat de meeste verstoven deeltjes ontstaan ten gevolge van botsingen diep in het kristal. Gebruik makend van de voorkeursrichtingen, waarin deze laatstgenoemde verstuiving optreedt, kon de eerstgenoemde verstuiving gedetecteerd worden. Zij werd, volgens verwachting, gevonden in richtingen loodrecht op de ionenbundel. De bijdrage van dit verstuivingsmechanisme tot de totale verstuivingsverhouding werd geschat op 0,7, in overeenstemming met de theoretische waarde, die geldig moet zijn voor de grote botsingsstralen behorend bij de lage energie-overdrachten.

In hoofdstuk IV wordt beschreven hoe de temperatuur van het koper de verstuivingsverhouding beinvloedt (40—900°K). Dit wordt eerst nagegaan voor temperaturen boven kamertemperatuur uitgaande van de resultaten van een theorie van J. B. Sanders over de dracht van een focusserende stoot in de [100] richting. De kleine waarde van deze dracht is in overeenstemming te brengen met een vrijwel temperatuur-onafhankelijke verstuiving.
Metingen van verstuivingsverhoudingen bij kopertemperaturen onder 150°K laten een geheel ander beeld zien. Voor Ar^+ ionen wordt weliswaar ook een constante verstuivingsverhouding gevonden, maar voor Ne^+ ionen treedt zowel onder 150°K als onder 50°K een sterke afname van de verstuivingsverhouding op. Aangenomen wordt dat de drachten van de [110] - focusserende stoten sterk verkort worden tengevolge van een toegenomen wanorde in het kristal. De langzamere diffusie van interstitiële koperatomen onder de genoemde temperaturen kan hiervoor verantwoordelijk gesteld worden. Uit de temperaturen, waar de sterkste verandering van de verstuivingsverhouding gevonden wordt, kan dan een activeringsenergie voor de diffusie bepaald worden. Deze blijkt 0,29 eV en ongeveer 0,1 eV te zijn, in goede overeenstemming met de theoretische waarden voor de twee stabiele interstitiële configuraties in koper, die door K. H. Bennemann bepaald werden.
Voor 100°K naar 50°K neemt de verstuivingsverhouding toe. Dit werd toegeschreven aan een toename van de Ne concentratie. Bij ontgassing van bij 50°K beschoten koper, bleek inderdaad meer gas

vrij te komen. Het eerder genoemde verschil in gedrag tussen Ar en Ne wordt toegeschreven aan de snellere diffusie van Ne.

Hoofdstuk V beschrijft een studie over de productie van snelle secundaire deeltjes bij Ar$^+$ beschieting van koper. "Gereflecteerde" atomen werden gemeten met een secundaire emissie detector. Met behulp van een gepulste ionenbundel kon de snelheid van de "gereflecteerde" deeltjes bepaald worden. Hieruit bleek dat het voornamelijk snelle Ar atomen waren, verstrooid tijdens één botsing met een Cu atoom. De opbrengst aan "gereflecteerden" bleek dan ook snel met de hoek van inval toe te nemen, tot 1 % van de primaire ionenbundel bij zeer schuine inval. Met monokristallen werden ook relatief lage opbrengsten gevonden voor een invalsrichting van de ionen, die overeenkomt met een laag geïndiceerde kristalrichting. Het effect is echter kleiner dan dat voor verstuiving (hoofdstuk I). Dit wijst er op dat de snelle deeltjes niet alleen afkomstig zijn van verstrooiingen aan de oppervlakte atomen. Anderzijds liggen de verstrooiende Cu atomen toch weer niet zo diep als degene die bij verstuiving een rol spelen.

Het maximum in het aantal "gereflecteerde" atomen werd gevonden bij een "reflectie hoek" van 70°, onafhankelijk van de hoek van inval van de primaire ionen. Dit maximum zal bepaald worden door het reliëf van het target oppervlak (hoofdstuk II). Op grond hiervan mag verwacht worden dat vrij veel secundaire deeltjes opnieuw het target binnen dringen. Hierdoor kan een extra verstuiving optreden, die geschat werd op 10 % van de verstuiving, die voor perfect vlakke oppervlakken zou gelden.